



1 Terrestrial Ecosystem Process Model Biome-BGCMuSo: 2 Summary of improvements and new modeling possibilities

3 Dóra Hidy¹, Zoltán Barcza², Hrvoje Marjanović³, Maša Zorana Ostrogović Sever³, Laura
4 Dobor², Györgyi Gelybó⁴, Nándor Fodor⁵, Krisztina Pintér¹, Galina Churkina⁶, Steven
5 Running⁷, Peter Thornton⁸, Gianni Bellocchi⁹, László Haszpra^{10,13}, Ferenc Horváth¹¹, Andrew
6 Suyker¹², Zoltán Nagy¹

7
8 ¹ MTA-SZIE Plant Ecology Research Group, Szent István University, Páter K. u.1., H-2103 Gödöllő, Hungary

9 ² Department of Meteorology, Eötvös Loránd University, Pázmány P. sétány 1/A., H-1117 Budapest, Hungary

10 ³ Croatian Forest Research Institute, Department for Forest Management and Forestry Economics, Cvjetno
11 naselje 41, 10450 Jastrebarsko, Croatia

12 ⁴ Institute for Soil Sciences and Agricultural Chemistry, Centre for Agricultural Research, Hungarian Academy
13 of Sciences, Herman O. út 15., H-1163 Budapest, Hungary

14 ⁵ Agricultural Institute, Centre for Agricultural Research, Hungarian Academy of Sciences, Brunszvik u. 2., H-
15 2462

16 Martonvásár, Hungary

17 ⁶ Institute for Advanced Sustainability Studies e.V., Berliner Strasse 130, D-14467 Potsdam, Germany

18 ⁷ Numerical Terradynamic Simulation Group, Department of Ecosystem and Conservation Sciences University
19 of Montana, Missoula, MT 59812 USA

20 ⁸ Climate Change Science Institute / Environmental Sciences Division, Oak Ridge National Laboratory, Oak
21 Ridge, TN 37831-6335, USA

22 ⁹ UREP, INRA, 63000 Clermont-Ferrand, France

23 ¹⁰ Hungarian Meteorological Service, H-1675 Budapest, P.O.Box 39, Hungary

24 ¹¹ Institute of Ecology and Botany, Centre for Ecological Research, Hungarian Academy of Sciences, Alkotmány
25 u. 2-4., H-2163 Vácraátót, Hungary

26 ¹² School of Natural Resources, University of Nebraska-Lincoln, 806 Hardin Hall, Lincoln, Nebraska 68588,
27 USA

28 ¹³ Geodetic and Geophysical Institute, MTA Research Centre for Astronomy and Earth Sciences, H-9400
29 Sopron, Csatkaí Endre utca 6-8., Hungary

30 *Correspondence to:* Dóra Hidy (dori.hidy@gmail.com)

31



1 **Abstract.** The process-based biogeochemical model Biome-BGC was enhanced to improve its ability to
2 simulate carbon, nitrogen and water cycles of various terrestrial ecosystems under contrasting management
3 activities. Biome-BGC version 4.1.1 was used as base model. Improvements included addition of new modules
4 such as the multilayer soil module, implementation of processes related to soil moisture and nitrogen balance,
5 soil moisture related plant senescence, and phenological development. Vegetation management modules with
6 annually varying options were also implemented to simulate management practices of grasslands (mowing,
7 grazing), croplands (ploughing, fertilizer application, planting, harvesting), and forests (thinning). New carbon
8 and nitrogen pools have been defined to simulate yield and soft stem development of herbaceous ecosystems.
9 The model version containing all developments is referred to as Biome-BGCMuSo (Biome-BGC with multi-
10 layer soil module). Case studies on a managed forest, cropland and grassland are presented to demonstrate the
11 effect of model developments on the simulation of plant growth as well as on carbon and water balance.

12

13 **Keywords:** model development, Biome-BGC, biogeochemical model, management, soil water content, drought
14 stress

15



1 1 Introduction

2 The development of climate models has led to the construction of Earth System Models (ESMs) with varying
3 degrees of complexity where the terrestrial carbon cycle is included as a dynamic submodel (Ciais et al., 2013).
4 In ESMs, the atmospheric concentration of carbon dioxide (CO₂) is no longer prescribed by the emission
5 scenarios but it is calculated dynamically as a function of anthropogenic CO₂ emission and the parallel ocean and
6 land surface carbon uptake. Focusing specifically on land surface, the carbon balance of terrestrial vegetation can
7 be quantified by state-of-the-art biogeochemical models and are integral parts of the ESMs.

8 At present, there is no consensus on the future trajectory of the terrestrial carbon sink (Fig. 6.24 in Ciais et al.,
9 2013). Some ESMs predict saturation of the land carbon sink in the near future while others show that the uptake
10 will keep track with the increasing CO₂ emission. This means a considerable uncertainty related to the climate-
11 carbon cycle feedback (Friedlingstein et al., 2006; Friedlingstein and Prentice, 2010). The wide range of model
12 data related to the land carbon sink means that the current biogeochemical models have inherent uncertainties
13 which must be addressed.

14 Biogeochemical models need continuous development to include empirically discovered processes and
15 mechanisms e.g. acclimation processes describing the dynamic responses of plants to the changing
16 environmental conditions (Smith and Dukes, 2012), regulation of stomatal conductance under elevated CO₂
17 concentration (Franks et al., 2013), drought effect on vegetation functioning (van der Molen et al., 2011), soil
18 moisture control on ecosystem functioning (Yi et al., 2010) and other processes. Appropriate description of
19 human intervention is also essential to adequately quantify lateral carbon fluxes and net biome production
20 (Chapin et al., 2006). Keeping track with the new measurement-based findings is a challenging task but
21 necessary to improve our ability to simulate the terrestrial carbon cycle more accurately.

22 The process-based biogeochemical model Biome-BGC is the focus of this study. The model was developed by
23 the Numerical Terradynamic Simulation Group (NTSG), at the University of Montana
24 (<http://www.ntsug.umt.edu/project/biome-bgc>), and is widely used to simulate carbon (C), nitrogen (N) and water
25 fluxes of different terrestrial ecosystems such as deciduous and evergreen forests, grasslands and shrublands
26 (Running and Hunt, 1993; Thornton, 1998; Thornton et al., 2002; Churkina et al., 2009; Hidy et al., 2012).

27 Biome-BGC is one of the earliest biogeochemical models that include an explicit N cycle module. It is now clear
28 that climate-carbon cycle interactions are affected by N availability and the CO₂ fertilization effect can be
29 limited by the amount of N in ecosystems (Friedlingstein and Prentice, 2010; Ciais et al., 2013). Therefore, the
30 explicit simulation of the N cycle is an essential part of these biogeochemical models (Thomas et al., 2013).

31 Several researchers used and modified Biome-BGC in the past. Without being exhaustive, here we review some
32 major applications on forest ecosystems, grasslands, croplands, urban environment, and we also list studies that
33 focused on the spatial application of the model on regional and global scales.

34 Vitousek et al. (1988) studied the interactions in forest ecosystems such as succession, allometry and input-
35 output budgets using Biome-BGC. Nemani and Running (1989) tested the theoretical atmosphere-soil-leaf area
36 hydrologic equilibrium of forests using satellite data and model simulation with Biome-BGC. Korol et al. (1996)
37 tested the model against observed tree growth and simulated the 5-year growth increments of 177 Douglas-fir



1 trees growing in uneven-aged stands. Kimball et al. (1997) used Biome-BGC to simulate the hydrological cycle
2 of boreal forest stands. Thornton et al. (2002) developed the model to simulate forest fire, harvest and replanting.
3 Churkina et al. (2003) used Biome-BGC to simulate coniferous forest carbon cycle in Europe. Pietsch et al.
4 (2003) presented developments of Biome-BGC where water infiltration from groundwater and the effect of
5 seasonal flooding were taken into account in floodplain forest areas. Bond-Lamberty et al. (2007) developed
6 Biome-BGC-MV to enable simulation of forest species succession and competition between vegetation types.
7 Vetter et al. (2005) used Biome-BGC to simulate the effect of human intervention on coniferous forest carbon
8 balance. Schmid et al. (2006) assessed the accuracy of Biome-BGC to simulate forest carbon balance in Central
9 Europe. Tatarinov and Cienciala (2006) further improved the Biome-BGC facilitating management practices in
10 forest ecosystems (including thinning, felling, and species change). Merganičová et al. (2005) and Petritsch et al.
11 (2007) implemented forest management in the model including thinning and harvest. Bond-Lamberty et al.
12 (2007) implemented elevated groundwater effect on stomatal conductance and decomposition in Biome-BGC.
13 Chiesi et al. (2007) evaluated the applicability of Biome-BGC in drought-prone Mediterranean forests. Turner et
14 al. (2007) used Biome-BGC to estimate the carbon balance of a heterogeneous region in the western United
15 States. Ueyama et al. (2010) used the model to simulate larch forest biogeochemistry in East Asia. Maselli et al.
16 (2012) used the model to estimate olive fruit yield in Tuscany, Italy. Hlásny et al. (2014) used Biome-BGC to
17 simulate the climate change impacts on selected forest plots in Central Europe.
18 Di Vittorio et al. (2010) developed Agro-BGC to simulate the functioning of C4 perennial grasses including a
19 new disturbance handler and a novel enzyme-driven C4 photosynthesis module.
20 Wang et al. (2005) applied Biome-BGC to simulate cropland carbon balance in China. Ma et al. (2011)
21 developed ANTHRO-BGC to simulate the biogeochemical cycles of winter crops in Europe including an option
22 for harvest and considering allocation to yield.
23 Trusilova and Churkina (2008) applied Biome-BGC to estimate the carbon cycle of urban vegetated areas.
24 Lagergren et al. (2006) used Biome-BGC to estimate the carbon balance of the total forested area in Sweden. Mu
25 et al. (2008) used Biome-BGC to estimate the carbon balance of China. Jochheim et al. (2009) presented forest
26 carbon budget estimates for Germany based on a modified version of Biome-BGC. Barcza et al. (2009, 2011)
27 used Biome-BGC to estimate the carbon balance of Hungary. Eastaugh et al. (2011) used Biome-BGC to
28 estimate the impact of climate change on Norway spruce growth in Austria. Biome-BGC was used within the
29 CARBOEUROPE-IP project as well as in several studies exploiting the related European scale simulation results
30 (e.g. Jung et al. 2007a, b; Vetter et al., 2008; Schulze et al., 2009; Ľupek et al., 2010; Churkina et al., 2010).
31 Hunt et al. (1996) used Biome-BGC in a global scale simulation and compared the simulated net primary
32 production (NPP) with satellite based vegetation index. Hunt et al. (1996) also used an atmospheric transport
33 model coupled with Biome-BGC to simulate surface fluxes to estimate the distribution of CO₂ within the
34 atmosphere. Churkina et al. (1999) used Biome-BGC in a global scale multimodel intercomparison to study the
35 effect of water limitation on NPP. Churkina et al. (2009) used Biome-BGC in a coupled simulation to estimate
36 the global carbon balance for the present and up to 2030. Biome-BGC is used in the Multiscale synthesis and
37 Terrestrial Model Intercomparison Project (MsTMIP) (Huntzinger et al., 2013; Schwalm et al., 2010) as part of
38 the North American Carbon Program.



1 In spite of its popularity and proven applicability, the model development temporarily stopped at version 4.2.
2 One major drawback of the model was its relatively poor performance in the simulation of the effect of
3 management practices. It is also known that anthropogenic effects exert a major role in the transformation of the
4 land surface in large spatial scales (Vitousek et al., 1998). Some structural problems also emerged like the
5 simplistic soil moisture module (using one soil layer), lack of new structural developments (see e.g. Smith and
6 Dukes, 2012), problems associated with phenology (Hidy et al., 2012), and lack of realistic response of
7 ecosystems to drought (e.g. senescence).
8 Our aim was to improve the model by targeting significant structural development, and to create a unified, state-
9 of-the-art version of Biome-BGC that can be potentially used in Earth System Models, as well as in situations
10 where management and water availability plays an important role (e.g. in semi-arid regions) in biomass
11 production. The success and widespread application of Biome-BGC can partly be attributed to the open source
12 nature of the model code. Following this tradition, we keep the developed Biome-BGC open source. In order to
13 support application of the model, a comprehensive User's Guide was also compiled (Hidy et al., 2015).
14 In the present work, the scientific basis of the developments is presented in detail followed by verification
15 studies in different ecosystems (forest, grassland and cropland) to demonstrate the effect of the developments on
16 the simulated fluxes and pools.

17 2 Study sites

18 Model developments were motivated by the need to improve model simulation for grasslands, croplands, and
19 forests. Here we demonstrate the applicability of the developed model at three sites on three different plant
20 functional types characterized by contrasting management, climate and site conditions.

21 2.1 Grassland/pasture

22 The large pasture near Bugacpuszta (46.69° N, 19.60° E, 111 m a.s.l.) is situated in the Hungarian Great Plain
23 covering an area of 1074 hectares. The study site (2 ha) has been used as pasture for the last 150 years according
24 to archive army maps from the 19th century. The soil surface is characterized by an undulating micro-topography
25 formed by winds within an elevation range of 2 m. The vegetation is highly diverse (species number over 80)
26 dominated by *Festuca pseudovina* Hack. ex Wiesb., *Carex stenophylla* Wahlbg., *Cynodon dactylon* L. Pers., *Poa*
27 spp.

28 The average annual precipitation is 562 mm and the annual mean temperature is 10.4 °C. According to the FAO
29 classification (Driessen et al., 2001) the soil type is chernozem with a rather high organic carbon content (51.5 g
30 kg⁻¹ for the 0-10 cm top soil; Balogh et al., 2011). The soil texture is sandy loamy sand (sand content 78%, silt
31 content 9% in 0-10 cm soil layer). The pasture belongs to the Kiskunság National Park and has been under
32 extensive grazing by a Hungarian grey cattle herd in the last 20 years. Stocking density was
33 0.23-0.58 animal ha⁻¹ during the 220-day-long grazing period between 2004 and 2012.

34 Carbon dioxide (CO₂) and latent heat flux (LHF) have been measured by the eddy-covariance (EC) technique.
35 Continuous measurements began in 2003 and they are used in this study as input and verification data (Nagy et
36 al., 2007, 2011). The EC station has a measurement height of 4 m and is equipped with a CSAT3 (Campbell



1 Scientific) sonic anemometer and a LI-7500 open path infrared gas analyzer (IRGA; LI-COR Inc., Lincoln, NE)
2 to measure fluxes of sensible and latent heat and CO₂. Several other sensors measure micrometeorological
3 variables including wind speed and direction, air temperature and relative humidity, precipitation, global,
4 reflected and net solar radiation, photosynthetically-active photon flux density (PPFD), reflected PPFD, soil heat
5 flux, soil temperature, and soil moisture. Soil water content was measured by CS616 (Campbell Scientific,
6 Shepshed, Leic's, UK) probes. Two probes were inserted horizontally at 3 and 30 cm depth and one was inserted
7 vertically averaging the soil water content of the upper 30 cm soil layer. For model evaluation measured soil
8 water content at 30 cm depth was used.

9 Data processing includes spike detection and removal following Vickers and Mahrt (1997) and linear detrending
10 to calculate fluctuations from the raw data. The flow disturbance effect of sensor heads is influenced by the angle
11 between the wind vector and horizontal plane, the so called angle of attack. To avoid errors caused by this error
12 our database is calibrated after van der Molen et al. (2004). The error caused by the inaccurate levelling of the
13 sonic anemometer is corrected by the planar fit method (Wilczak et al., 2001), in a slightly modified way.
14 Crosswind correction for sensible heat flux is done following Liu et al. (2001). The fluctuation in air density
15 influences the concentrations measured by the open path IRGA, which is not taken into account during the
16 measurements, but has to be done afterwards by the Webb-Pearman-Leuning correction (WPL; Webb et al.,
17 1980). To take into consideration the damping effect of sensor line averaging, separation distance between scalar
18 and wind sensor and the limited response time of both the anemometer and the LI-COR 7500 LI-COR Inc.,
19 Lincoln, NE, frequency response corrections were applied (Moore, 1986). Gap-filling and flux partitioning
20 method is based on the non-linear function between PPFD and daytime CO₂ fluxes, and temperature and night-
21 time CO₂ fluxes (Reichstein et al., 2005).

22 2.2 C4 cropland

23 Three production-scale cropland measurement sites were established in 2001 at the University of Nebraska
24 Agricultural Research and Development Center near Mead, Nebraska, USA, which are the part of the AmeriFlux
25 (<http://ameriflux.ornl.gov/>) and the FLUXNET global network (<http://fluxnet.ornl.gov/>). Mead1 (41.17° N,
26 96.48° W, 361 m a.s.l.; 48.7 ha) and Mead 2 (41.16° N, 96.47° W, 362 m a.s.l.; 52.4 ha) are both equipped with
27 center pivot irrigation systems. Mead3 (41.18° N, 96.44° W, 362 m a.s.l.; 65.4 ha) relies on rainfall. Maize is
28 planted each year at Mead1 while Mead2 and Mead3 are in a maize-soybean rotation.

29 On the Mead sites the annual average temperature is 10.1 °C and the mean annual precipitation total is 790 mm.
30 Soil at the site is deep silty clay loam consisting of four soil series: Yutan (fine-silty, mixed, superactive, mesic
31 Mollic Hapludalfs), Tomek (fine, smectitic, mesic Pachic Argialbolls), Filbert (fine, smectitic, mesic Vertic
32 Argialbolls), Filmore (fine, smectitic, mesic Vertic Argialbolls).

33 The CO₂ and energy fluxes are measured by an EC system using an omnidirectional three dimensional sonic
34 anemometer (Model R3, Gill Instruments Ltd., Lymington, UK), an open-path infrared CO₂/H₂O gas analyzer
35 (Model LI-7500: LI-COR Inc., Lincoln, NE) and a closed-path CO₂/H₂O system (Model LI-6262: LI-COR Inc.,
36 Lincoln, NE). The sensors were mounted 3 m above the ground when the canopy was shorter than 1 m, and later
37 moved to a height of 6 m until harvest when maize was planted (Suyker et al., 2004; Verma et al., 2005).



1 Raw EC data processing included correction of fluxes for inadequate sensor frequency response (i.e., tube
2 attenuation, sensor separation; Massman, 1991; Moore, 1986). Fluxes were adjusted for flow distortion (Nakai et
3 al., 2006) and the variation in air density due to the transfer of water vapour (Webb et al., 1980; Suyker et al.
4 2003).

5 Air temperature and humidity were measured at 3.0 m and 6.0 m height (Humitter50Y, Vaisala, Helsinki,
6 Finland). PPFD (LI 190SA Quantum Sensor, LI-COR Inc., Lincoln, NE), net radiation at 5.5 m height (Q*7.1,
7 Radiation and Energy Balance Systems Inc., Seattle, WA), and soil heat flux (0.06 m depth; Radiation and
8 Energy Balance Systems Inc.) were also measured (Verma et al., 2005). Soil water content measured at 0.1 m
9 depth was used in this study (ML2 Thetaprobe, Delta T Devices Ltd, Cambridge, UK).

10 Green leaf area index (LAI) was determined from destructive sampling. A LI-COR 3100 (LI-COR Inc., Lincoln,
11 NE) leaf area meter was used to measure sampled leaves. Each sampling was from six, 1-meter long row
12 samples from six parts of the field. Aboveground biomass was determined using destructive plant sampling.
13 Each sampling was from 1-meter long row samples from each of six different parts of the field. Plants were cut
14 off at ground level, brace roots were removed, and plants were placed in fine mesh bags. Plants were dried to
15 constant weight. Subsequently, the mass of green leaves, stems, reproductive organs, and senesced tissue were
16 determined on a per plant basis. Measured plant populations were used to convert from per plant-basis to a unit
17 ground area basis.

18 The Mead1 site was under no-till management prior to the harvest of 2005. Currently, there is a fall conservation
19 tillage for which approximately 1/3 of the crop residue is left on the surface. From 2010 to 2013, for a biomass
20 removal study, management at Mead2 was identical to Mead1 (continuous maize, fall conservation tillage, etc).
21 Management settings of the simulations were based on site records. In this study, Mead1 site is used for model
22 evaluation.

23 2.3 Deciduous broad-leaved forest

24 The Jastrebarsko site (45.62 °N 15.69 °E, 115 m a.s.l.) is a forest study site situated in a lowland oak forest that
25 is part of the state-owned Pokupsko basin forest complex, located approximately 35 km SW of Zagreb (Croatia).
26 Forest compartment where the EC tower for CO₂ flux measurement is located was a 37 years old mixed stand
27 dominated by *Quercus robur* L. (58 %) accompanied by other tree species, namely *Alnus glutinosa* (L.) Geartn.
28 (19%), *Carpinus betulus* L. (14%), *Fraxinus angustifolia* Vahl. (8%), and other (1%). *Corylus avellana* L. and
29 *Crateagus monogyna* Jacq. are common in the understory. Oak forests in this area are managed in 140 year long
30 rotations. Stands are thinned once every 10 years ending with regeneration cuts during the last 10 years of the
31 rotation (two or three), aimed at facilitating natural regeneration of the stand and continuous cover of the soil.
32 Annual mean temperature was 10.6 °C and average annual precipitation was 962 mm during the period of 1981–
33 2010 (data from the National Meteorological and Hydrological Service for the Jastrebarsko meteorological
34 station). The average annual depth to the groundwater ranges from 60 to 200 cm (Mayer, 1996). Groundwater
35 level in a 4 m deep piezometer was measured weekly during the vegetation season from 2008 onwards. During
36 winter and early spring, parts of the forest are waterlogged or flooded with stagnating water due to heavy soil.
37 Soil is mainly gleysol with low vertical water conductivity (Mayer, 1996), and according to the WRB, it is



1 classified as luvic stagnosol. The soil texture is dominantly clay with 18% of sand and 28% of silt fraction in the
2 0-30 cm top soil layer (Mayer, 1996).

3 Carbon dioxide and latent heat flux have been measured by the EC technique since September 2007 (Marjanović
4 et al., 2011a, b). The measurement height at the time of installation was 23 m above ground (3–5 m above the
5 top of the canopy). Since the forest stand grew, the measurement height was elevated to 27 m in April, 2011. The
6 EC system was made up of a sonic anemometer (81,000 V, R.M. Young, USA) and an open path IRGA (LI-
7 7500, LI-COR Inc., Lincoln, NE) with a sampling rate of 20 Hz. Meteorological measurements included soil
8 temperature, incoming short-wave radiation, incoming and outgoing PPF, net radiation, air temperature and
9 humidity, soil heat flux and total rainfall. Soil water content was measured at 0–30 cm depth using two time-
10 domain reflectometers (Marjanović et al., 2011a).

11 Raw data processing of EC data was made using EdiRe Data Software (University of Edinburgh, United
12 Kingdom) according to the methodology based on the EuroFlux protocol (Aubinet et al., 2000) with a further
13 adjustment such as the WPL correction (Webb et al., 1980). Quality assessment and quality check analysis (QA
14 and QC) have been applied according to Foken and Vichura (1996). Net ecosystem exchange (NEE) was
15 obtained after taking into account the storage term which was calculated using a profile system designed to make
16 sequential CO₂ concentration measurements (IRGA, SBA-4, PPSystems) from 6 heights in a 6 minute cycle.
17 Quality assessment and quality control was made according to Foken and Vichura (1996). Gap-filling of missing
18 data and NEE flux partitioning to gross primary production (GPP) and total ecosystem respiration (TER) was
19 made using online EC data gap filling and flux partitioning tools ([http://www.bgc-
20 jena.mpg.de/~MDIwork/eddyproc/](http://www.bgc-jena.mpg.de/~MDIwork/eddyproc/)) using the method of Reichstein et al. (2005).

21 Jastrebarsko forest stand characteristics data include diameter at breast height (dbh) and volume distribution by
22 tree species, weekly tree stem and height increment, tree mortality, phenology data, annual litterfall, litterfall C
23 and N content, fine root biomass, net annual root-derived carbon input, soil texture and carbon content
24 (Marjanović et al., 2011b; Ostrogović, 2013; Alberti et al., 2014). Data were used either as input in modeling
25 (e.g. groundwater level), for assessing some of the model parameters (e.g. phenology data) or model evaluation
26 (e.g. EC fluxes, tree increment measurements).

27 **3 Description of base model: Biome-BGC 4.1.1 MPI**

28 Our model developments started before Biome-BGC 4.2 was published. The starting point was Biome-BGC
29 v4.1.1 with modifications described in Trusilova et al. (2009). We refer to this model as Biome-BGC v4.1.1 MPI
30 version (MPI refers to the Max Planck Institute in Jena, Germany) or original Biome-BGC. Biome-BGC v4.1.1
31 MPI version was developed from the Biome-BGC family of models (Thornton, 2000). Biome-BGC is the
32 extension and generalization of the Forest-BGC model to describe different vegetation types including C3 and
33 C4 grasslands (Running and Coughlan, 1988; Running and Gower, 1991; Running and Hunt, 1993; Thornton,
34 2000; White et al., 2000; Trusilova et al., 2009).

35 Biome-BGC uses a daily time step and is driven by daily values of maximum and minimum temperatures,
36 precipitation, solar radiation, and daylight vapour pressure deficit (VPD). In addition to meteorological data
37 Biome-BGC uses site specific data (e.g. soil texture, site elevation, latitude), and ecophysiological data (e.g.



1 maximum stomatal conductance, specific leaf area, C:N mass ratios in different plant compartments, allocation
2 related parameters, etc.) to simulate the biogeochemical processes of the given biome. The main simulated
3 processes are photosynthesis, evapotranspiration, allocation, litterfall, C, N and water dynamics in the litter and
4 soil (Thornton, 2000).

5 The three most important blocks of the model are the phenological, the carbon flux, and the soil flux block. The
6 phenological block calculates foliage development and therefore affects the accumulation of C and N in leaf,
7 stem (if present), root and consequently the amount of litter. In the carbon flux block gross primary production
8 of the biome is calculated using Farquhar's photosynthesis routine (Farquhar et al., 1980) and the enzyme
9 kinetics model based on Woodrow and Berry (1988). Autotrophic respiration is separated into maintenance and
10 growth respirations. In addition to temperature, maintenance respiration is the function of the N content of living
11 plant biomass, while growth respiration is calculated proportionally to the carbon allocated to the different plant
12 compartments. The soil block describes the decomposition of dead plant material (litter) and soil organic matter,
13 N mineralization and N balance in general (Running and Gower, 1991). The soil block uses the so-called
14 converging cascade model (Thornton and Rosenbloom, 2005).

15 In Biome-BGC, the main parts of the ecosystem are defined as plant, soil and litter. Since Biome-BGC simulates
16 water, carbon and N cycles of C3 and C4 plants, the following main pools are defined: leaf (C, N and water),
17 fine root (C, N), soil (C, N and water) and litter (C, N). C and N pools have sub-pools (i.e., actual pools, storage
18 pools and transfer pools). Sub-pools contain the amount of C or N available on the simulation day. Storage sub-
19 pools store the amount that will appear next year (like a core or bud), while the transfer sub-pools store the
20 whole content of the storage pool after the end of the actual transfer period until the next one, and what will be
21 transferred gradually into the leaf carbon pool (like a germ) in the next transfer period.

22 The model simulation has two phases. The first is the spinup simulation (or in other words self-initialization or
23 equilibrium run), which starts with very low initial level of soil C and N and runs until a steady state is reached
24 with the climate in order to estimate the initial values of the state variables (Thornton, 2000; Thornton and
25 Rosenbloom, 2005). In the second phase, the normal simulation uses the results of the spinup simulation as
26 initial values for the C and N pools. This simulation is performed for a given, predetermined time period.

27 **4 Methodological results: model adjustments**

28 Some improvements focusing primarily on the development of the model to simulate carbon and water balance
29 of managed herbaceous ecosystems have already been published (Hidy et al., 2012). Previous model
30 developments included structural improvements on soil hydrology and plant phenology. Additionally, several
31 management modules were implemented in order to provide more realistic fluxes for managed grasslands. We
32 refer this model version as modified Biome-BGC (this is the predecessor of the current model).

33 Several developments have been made since the publication of the Hidy et al. (2012) study. The model that we
34 present in this study is referred to as Biome-BGCMuSo (abbreviated as BBGCMuSo, where MuSo refers to
35 MULTilayer SOil module). Currently, BBGCMuSo has several versions but hereafter only the latest version (4.0)
36 is discussed.



1 In this paper, we provide detailed documentation of all changes made in the model logic compared to the original
2 model (Biome-BGC v4.1.1). Here we briefly mention the previously published developments and we provide
3 detailed description concerning the new features. In order to illustrate the effect and the importance of the
4 developments, model evaluations are presented for three contrasting sites equipped with EC measurement
5 systems in Section 5.

6 Due to the modifications of the model structure and the implementation of the new management modules, it was
7 necessary to modify the structure of the input and output files of the model. Technical details are discussed in the
8 User's Guide of BBGCMuSo (Hidy et al., 2015;
9 http://nimbus.elte.hu/bbgc/files/Manual_BBGC_MuSo_v4.0.pdf).

10 We summarized the model adjustments in Table 1. Within the table the implemented processes are grouped for
11 clarity. Below we document the adjustments in detail.

12 **4.1 Multilayer soil**

13 The predecessor of Biome-BGC (FOREST-BGC) was developed to simulate the carbon and water budgets of
14 forests where soil moisture limitation is probably less important due to the deeper rooting zone. Therefore, its
15 soil sub-model was simple and included only a one-layer budget model. Due to the recognized importance of soil
16 hydrology on the carbon and water balance, state-of-the-art biogeochemical models include multilayer soil
17 module (e.g. Schwalm et al., 2015).

18 In order to improve the simulation quality of water and carbon fluxes with Biome-BGC, a seven-layer soil sub-
19 model was implemented. Seven layers provide an optimal compromise between simulation accuracy and
20 computational cost. In accordance with the soil layers, we also defined new fluxes within the model. Note that in
21 the Hidy et al. (2012) publication the developed Biome-BGC had only 4 soil layers, so the 7-layer module is an
22 improvement.

23 The first layer is located at depth of 0-10 cm; the second is at 10-30 cm, the third is at 30-60 cm, the fourth is at
24 60-100 cm, the fifth is at 100-200 cm, and the sixth is at 200-300 cm. The bottom (7th, hydrologically and
25 thermally inactive) layer is located at depth 300-1000 cm. The depth of a given soil layer is represented by the
26 center of the given layer. Below 5 meters the soil temperature can be assumed equal to the annual average air
27 temperature of the site (Florides and Kalogirou, 2016). Furthermore, in the bottom layer we assume that soil
28 water content (SWC) is equal to the field capacity (constant value) and soil mineral content has a small, constant
29 value (1 kg N ha^{-1} within the 7 m deep soil column). The percolated water (and soluble N) to the bottom,
30 hydrologically inactive layer is a net loss, while the water (and soluble N) diffused upward from the bottom layer
31 is a net gain for the simulated soil system.

32 Soil texture and soil bulk density can be defined by the user layer by layer. If the maximum rooting zone
33 (defined by user) is greater than 3 m, the roots reach the constant boundary soil layer and water uptake can occur
34 from that layer, as well. In previous BBGCMuSo model versions, the soil texture was constant with depth and
35 the maximum possible rooting depth was 5 m.



1 4.1.1 Soil thermodynamics

2 Since some of the soil processes depend on the actual soil temperature (e.g. decomposition of soil organic
 3 matter), it is necessary to calculate soil temperature for each active layer. Given the importance of soil
 4 temperature (e.g. Sándor et al., 2016), the soil module was also reconsidered in BBGCMuSo. The daily soil
 5 surface temperature is determined after (Zheng et al., 1993). The basic equations are detailed in Hidy et al.
 6 (2012). An important modification in BBGCMuSo is that the average temperature of the top soil layer (with
 7 thickness of 10 cm) is not equal to the above mentioned daily surface temperature. Instead, temperature of the
 8 active layers is estimated based on an empirical equation with daily time step.

9 Two optional empirical estimation methods are implemented in BBGCMuSo. The first is a simple method,
 10 assuming a logarithmic temperature gradient between the surface and the constant temperature boundary layer.
 11 This is an improvement compared to the modified Biome-BGC where a linear gradient was assumed. The second
 12 method is based on the soil temperature estimation method of the DSSAT model family (Ritchie 1998) and the
 13 4M model (Sándor and Fodor, 2012).

14 4.1.2 Soil hydrology

15 The C and the hydrological cycles of the ecosystems are strongly coupled due to interactions between soil
 16 moisture and stomatal conductance, soil organic matter decomposition, N mineralization and other processes.
 17 Accurate estimation of the soil water balance is thus essential.

18 Among soil hydrological processes, the original Biome-BGC only takes into account plant uptake, canopy
 19 interception, snowmelt, outflow (drainage) and bare soil evaporation. We have added the simulation of runoff,
 20 diffusion, percolation, pond water formation and enhanced the simulation of the transpiration processes in order
 21 to improve the soil water balance simulation. Optional handling of seasonally changing groundwater depth (i.e.,
 22 possible flooding due to elevated water table) is also implemented. In the Hidy et al. (2012) study, only runoff,
 23 diffusion and percolation were implemented (the simulation of these processes has been further developed since
 24 then). Pond water formation and simulation of groundwater movement are new features in BBGCMuSo 4.0.

25 Estimation of characteristic soil water content values

26 There are four significant characteristic points of the soil water retention curve: saturation, field capacity,
 27 permanent wilting point and hygroscopic water. Beside volumetric SWC, soil moisture status can also be
 28 described by soil water potential (PSI; MPa). The Clapp-Hornberger parameter (B; dimensionless) and the bulk
 29 density (BD; g cm⁻³), are also important in soil hydrological calculations (Clapp and Hornberger, 1978). Soil
 30 texture information (fraction of sand and silt within the soil; clay fraction is calculated by the model internally as
 31 a residual) for each soil layers are input data for BBGCMuSo. Based on soil texture other soil properties
 32 (characteristic points of SWC, B, BD) can be estimated internally by the model using pedotransfer functions
 33 (Fodor and Rajkai, 2011). The default values are listed in Table 2, which can be adjusted by the user within their
 34 plausible ranges.

35 As in the original Biome-BGC, the PSI at saturation is the function of soil texture in BBGCMuSo:

$$36 \text{ PSI}_{\text{sat}} = -\left\{ \exp\left[(1.54 - 0.0095 \cdot \text{SAND} + 0.0063 \cdot \text{SILT}) \cdot \ln(10) \right] \cdot 9.8 \cdot 10^{-5} \right\} \quad (1)$$



1 where SAND and SILT are the sand and silt percent fractions of the soil, respectively. In BBGCMuSo, PSI for
2 unsaturated soils is calculated from SWC using the saturation value of SWC (SWC_{sat}) and the B parameter:

$$3 \quad \text{PSI} = \exp\left(\frac{\text{SWC}_{\text{sat}}}{\text{SWC}} \cdot \ln(B)\right) \cdot \text{PSI}_{\text{sat}}, \quad (2)$$

4 Pond water and hygroscopic water

5 In case of intensive rainfall events, when not all of the precipitation can infiltrate, pond water is formulated at the
6 surface. Water from the pond can infiltrate into the soil after water content of the top soil layer decreases below
7 saturation. Evaporation of the pond water is assumed to be equal to potential soil evaporation.

8 SWC (as well as C and N content) is not allowed to become negative. The theoretical lower limit of SWC is the
9 hygroscopic water, i.e., the water content of air-dried soil. Therefore, in case of large calculated
10 evapotranspiration (calculated based on the Penman-Monteith equation as driven by meteorological data) and
11 dry soil, the soil water pool of the top layer can be depleted (approaching hygroscopic water content). In this
12 case evaporation and transpiration fluxes are limited in BBGCMuSo. Hygroscopic water content is also the
13 lower limit in decomposition calculations (see below).

14 *Runoff*

15 Our runoff simulation method is semi-empirical and uses the precipitation amount and the Soil Conservation
16 Service (SCS) runoff curve number (Williams, 1991). If the precipitation is greater than a critical amount which
17 depends on the water content of the topsoil, a fixed part of the precipitation is lost due to runoff and the rest
18 infiltrates into the soil. The runoff curve number can be set by the user or can be estimated by the model (Table
19 2).

20 Percolation and diffusion

21 In BBGCMuSo, two calculation methods of vertical soil water movement are implemented. The first method is
22 based on Richards' equation (Chen and Dudhia, 2001; Balsamo et al., 2009) Detailed description and equations
23 for this method can be found in Hidy et al. (2012). The second method is the so-called 'tipping bucket method'
24 (Ritchie, 1998) which is based on semi-empirical estimation of percolation and diffusion fluxes and has a long
25 tradition in crop modelling.

26 In case of the first method hydraulic conductivity and hydraulic diffusivity are used in diffusion and percolation
27 calculations. These variables change rapidly and significantly upon changes in SWC. Though the main processes
28 are calculated on daily time-step within the model, the simulation of the soil hydrological parameters required
29 finer temporal resolution; therefore a nested variable time-step-based calculation was introduced into the soil
30 hydrology sub-module in case of the first calculation method (in case of the tipping bucket method, a daily time-
31 step is used).

32 In BBGCMuSo, the time-step (TS; seconds) of the soil water module integration is dynamically changed. In
33 contrast to the modified Biome-BGC (Hidy et al., 2012) the TS is based on the theoretical maximum of soil
34 water flux instead of the amount of precipitation.

35 As a first step we calculate water flux data for a short, 1-second TS for all soil layers based on their actual SWC.
36 The most important problem here is the selection of the optimal TS: too small TS values result in slow model
37 run, while too large TS values lead to overestimation of water fluxes. TS is estimated based on the magnitude of



1 the maximal soil moisture content change in 1 second (ΔSWC_{\max} ; $m^3 m^{-3} s^{-1}$). Equation (3)-(4) describes the
 2 calculation of TS:

$$3 \quad TS = 10^{EXPON} \quad (3)$$

4 where

$$5 \quad \begin{aligned} EXPON &= \text{abs}[LV + (DL + 3)] \text{ if } DL + LV < 0 \\ EXPON &= 0 \quad \quad \quad \text{if } DL + LV \geq 0 \end{aligned} \quad (4)$$

6 LV is the rounded local value of the maximal soil moisture content change, and DL is the discretization level,
 7 which can be 0, 1 or 2 (low, medium or high discretization level which can be set by the user).

8 Therefore, if the magnitude of ΔSWC_{\max} is $10^{-3} m^3 m^{-3} s^{-1}$ (e.g. SWC increases from $0.400 m^3 m^{-3}$ to
 9 $0.401 m^3 m^{-3}$ in 1 second), then LV is -3, so TS is $100 = 1$ second (if $DL=0$). The 1-second TS is necessary if
 10 ΔSWC_{\max} is above $10^{-1} m^3 m^{-3} s^{-1}$. Using daily TS proved to be adequate when ΔSWC_{\max} was below
 11 $10^{-8} m^3 m^{-3} s^{-1}$.

12 After calculating the first TS (TSstep1 = 1 seconds), water fluxes are determined by using the pre-calculated
 13 time steps, and the SWC of the layers are updated accordingly. In the next n steps the calculations are repeated
 14 until reaching a threshold (86400, the number of the seconds in a day). This method helps to avoid the
 15 overestimation of the water fluxes while also decreasing the computation time of the model.

16 Groundwater

17 Poorly drained forests (e.g. in boreal regions or in lowland areas) are special ecosystems where groundwater and
 18 flooding play an important role in soil hydrology and plant growth (Bond-Lamberty et al., 2007; Pietsch et al.,
 19 2003). In order to enable groundwater effects (vertically varying soil water saturation), we implemented an
 20 option in BBGCMuSo to supply external information about the depth of the water table. Groundwater depth is
 21 controlled by prescribing the depth of saturated zone (groundwater) within the soil. We note that the
 22 groundwater implementations by Pietsch et al. (2003) and by Bond-Lamberty et al. (2007) are different from our
 23 approach as they calculate water table depth internally by the modified Biome-BGC. During the spinup phase
 24 of the simulation, the model can only use daily average data for one typical simulation year (i.e., multi-annual
 25 mean water table depth). During the normal phase, the model can read daily groundwater information defined
 26 externally.

27 The handling of the externally supplied, near-surface groundwater information is done as follows. If the upward
 28 moving water table reaches the bottom border of a simulated soil layer, part of the given layer becomes "quasi-
 29 saturated" (99% of the saturation value) and thus the average soil moisture content of the given layer increases.
 30 If the water table reaches the upper border of the given soil layer, then the given layer becomes quasi-saturated.
 31 The quasi-saturation state allows for the downward flow of water through a saturation soil layer, particularly
 32 through the last layer. This approach was necessary because of the discrete size of soil layers and the fact that the
 33 input groundwater level data constitute a net groundwater level. Namely, groundwater level is partly affected by
 34 lateral groundwater flows (which are unknown) and corresponding changes in hydraulic pressure that can push
 35 the water up; as well it is partly affected by draining of the upper soil layers. While soil is draining it is possible
 36 that the groundwater level remains unchanged, or that its level decreases slower because the drained water from
 37 the upper layer replaces the water that leaves the system (i.e., drains to below 10 m, which is the bottom of the



1 last soil layer). With implementation of quasi-saturation state we allowed for the water to flow through saturated
 2 layers, in particular through the bottom one. Otherwise the water could become “trapped” because the model
 3 routine could not allow downward movement of water from an upper soil layer to a lower layer that is already
 4 saturated (because that layer would have already been “full”).
 5 Groundwater level affects soil water content and in turn affects stomatal conductance and soil organic matter
 6 decomposition (see below).

7 4.1.3 Root distribution

8 Water becomes available to the plant through water uptake by the roots. The maximum depth of the rooting zone
 9 is a user-defined parameter in the model. For herbaceous vegetation, the temporally changing depth of the root is
 10 simulated based on an empirical, sigmoid function (Campbell and Diaz, 1988). In forests, fine root growth is
 11 assumed to occur in the entire root zone and rooting depth does not change with time. This latter logic is used
 12 due to the presence of coarse roots in forests which are assumed to change depth slowly (in juvenile forests this
 13 approach might be problematic).

14 In order to weight the relative importance of the soil layers (i.e., to distribute total transpiration or root
 15 respiration among soil layers), it is necessary to calculate the distribution of roots in the soil layers. The
 16 proportion of the total root mass in the given layer (R_{layer}) is calculated based on empirical exponential root
 17 profile approximation after Jarvis (1989):

$$18 \quad R_{\text{layer}} = f \cdot \left(\frac{\Delta z_{\text{layer}}}{z_r} \right) \cdot \exp \left[-f \cdot \left(\frac{z_{\text{layer}}}{z_r} \right) \right] \quad (5)$$

19 In Eq. (5), f is an empirical root distribution parameter (its proposed value is 3.67 after Jarvis, 1989), Δz_{layer} and
 20 z_{layer} is the thickness and the midpoint of the given soil layer, respectively, and z_r is the actual rooting depth.

21 Rooting depth and root distribution are taken into account by all ecophysiological processes which are affected
 22 by soil moisture content (transpiration), soil carbon content (maintenance respiration) and soil N content
 23 (decomposition).

24 4.1.4 Nitrogen budget

25 In previous model versions, uniform distribution of mineral N was assumed within the soil profile. In
 26 BBGCMuSo, we hypothesize that varying amounts of mineralized N are available within the different soil layers
 27 and are available for root uptake and other losses. The change of soil mineral N content is calculated layer by
 28 layer in each day. In the root zone (i.e., within soil layers containing roots), the changes of mineralized N-content
 29 are caused by soil processes (decomposition, microbial immobilization, denitrification), plant uptake, leaching,
 30 atmospheric deposition and biological N fixation. The produced/consumed mineralized N (calculated by
 31 decomposition and daily allocation functions) is distributed within the layers depending on their soil mineral N
 32 content. Mineralized N from atmospheric N deposition (N_{dep}) increases the N content of the first (0-10 cm) soil
 33 layer. Biological N fixation is divided between root zone layers as a function of the root fraction in the given
 34 layer. In soil layers without roots, N content is affected by transport (e.g. leaching) only. Leaching is calculated
 35 based on empirical function using the proportion of soluble N that is subject to mobilization (an adjustable



1 ecophysiological parameter in the model), mineral N content and the water fluxes (percolation and diffusion) of
2 the different soil layers.
3 There is an additional mechanism for N loss within the soil. According to the model logic (Thornton and
4 Rosenbloom, 2005) if there is excess mineral nitrogen in the soil following microbial immobilization and plant
5 N uptake, it is subject to volatilization and denitrification as a constant proportion of the excess mineral nitrogen
6 pool for a given day. In the original Biome-BGC (v4.1.1) this proportion was defined by a fixed parameter
7 within the model code. In Biome-BGC v4.2 two parameters were introduced that control bulk denitrification:
8 one for the wet and one for dry case (the wet case is defined when SWC is greater than the 95% of saturation). In
9 BBGCMuSo we implemented the Biome-BGC v4.2 logic which means that these values can be adjusted as part
10 of the ecophysiological model parameterization

11 4.1.5 Soil moisture stress index

12 Stomatal closure occurs due to low relative atmospheric moisture content (high VPD), and insufficient soil
13 moisture (drought stress; Damour et al., 2010) but also due to anoxic conditions (e.g. presence of elevated
14 groundwater or high soil moisture content during and after large precipitation events; Bond-Lamberty et al.,
15 2007). The original Biome-BGC had a relatively simple soil moisture stress function which was not adjustable
16 and was unable to consider anoxic conditions.

17 In order to create a generalized model logic for BBGCMuSo, the soil moisture limitation calculation was
18 improved, and the use of the stress function on stomatal conductance (and consequently transpiration and
19 senescence) calculations was extended taking into account both types of limitations mentioned above (limit1:
20 drought, limit2: anoxic condition close to soil saturation). The start and end of the water stress period are
21 determined by comparing actual and predefined, characteristic points of SWC and calculating a novel soil
22 moisture stress index (SMSI; dimensionless). Characteristic points of soil water status can be defined using
23 relative SWC (relative SWC to field capacity in case of limit1 and to saturation in case of limit2) or soil water
24 potential (see Section 3.4 of Hidy et al., 2015).

25 SMSI is the function of normalized soil water content (NSWC) (in contrast to original model, where SMSI was
26 the function of soil water potential). NSWC is defined by the following equation:

$$27 \text{NSWC} = \frac{\text{SWC} - \text{SWC}_{\text{wp}}}{\text{SWC}_{\text{sat}} - \text{SWC}_{\text{wp}}}, \text{ if } \text{SWC}_{\text{wp}} < \text{SWC} \quad , \quad (6)$$
$$\text{NSWC} = 0 \quad , \text{ if } \text{SWC}_{\text{wp}} \geq \text{SWC}$$

28 where SWC is the soil water content of the given soil layer ($\text{m}^3 \text{ m}^{-3}$), SWC_{wp} and SWC_{sat} are the wilting point
29 and the saturation value of soil water content, respectively. Parameters can either be set by the user or calculated
30 by the model internally (see Table 2).

31 The NSWC and the soil water potential as function of SWC are presented in Fig. 1 for three different soil types:
32 sand soil (SAND: 90%, SILT: 5%), sandy clay loam (SAND: 50%, SILT: 20%), and clay soil (SAND: 8%,
33 SILT: 45%).

34 According to our definition SMSI is a function of NSWC and can vary between 0 (maximum stress) and 1
35 (minimum stress).



1 The general form of SMSI is defined by the following equations:

$$\begin{aligned} \text{SMSI} &= \frac{\text{NSWC}}{\text{NSWC}_{\text{crit1}}}, \quad \text{if } \text{NSWC} < \text{NSWC}_{\text{crit1}} \\ 2 \quad \text{SMSI} &= 1, \quad \text{if } \text{NSWC}_{\text{crit1}} < \text{NSWC} \leq \text{NSWC}_{\text{crit2}} \\ \text{SMSI} &= \frac{1 - \text{NSWC}}{1 - \text{NSWC}_{\text{crit2}}}, \quad \text{if } \text{NSWC}_{\text{crit2}} < \text{NSWC} \end{aligned} \quad (7)$$

3 where $\text{NSWC}_{\text{crit1}}$ and $\text{NSWC}_{\text{crit2}}$ ($\text{NSWC}_{\text{crit1}} < \text{NSWC}_{\text{crit2}}$) are the characteristic points of the normalized soil
4 water curve, calculated from the relative soil water content or soil water potential values defined by
5 ecophysiological parameters. Conversion from relative values to NSWC is made within the model. Characteristic
6 point $\text{NSWC}_{\text{crit1}}$ is used to control drought related limitation, while $\text{NSWC}_{\text{crit2}}$ is used to control excess water
7 related limitation (e.g. anoxic soil related stomatal closure).

8 The shape of the soil stress function in the original model (based on soil water potential) and in BBGCMuSo
9 (based on NSWC) are presented in Fig. 2.

10 The value of the SMSI is zero in case of full soil water stress (below the wilting point). It starts to increase at the
11 wilting point (which depends on soil type; Table 1) and reaches its maximum (1) at the SWC where water stress
12 ends. This latter characteristic value can be set by the user. In this example (Fig. 2), field capacity was used as
13 the characteristic value. The new feature of the BBGCMuSo is that beyond the optimal soil moisture content
14 range, the soil stress can decrease again (i.e., increasing stress) due to saturation. This second characteristic value
15 (limit2) can also be set by a model parameter. In the example of Fig. 2 95% of the saturation value was used as
16 the second characteristic value.

17 The model requires only a single soil moisture stress function to calculate stomatal conductance, while soil water
18 status is calculated layer by layer. Therefore, an average stress function for the total rootzone is necessary, which
19 is the average of the layer factors weighted by root fraction in each layer.

20 Beside stomatal conductance, SMSI is used in the transpiration calculation in the multilayer soil. Instead of the
21 averaged soil water status of the whole soil column (as in original Biome-BGC), in BBGCMuSo, the
22 transpiration flux is calculated layer by layer. The transpiration flux of the ecosystem is assumed to be equal to
23 the total root water uptake on a given day (TRP_{sum}). The transpiration calculation is based on the Penman-
24 Monteith equation using stomatal conductance (this feature is the same as in the original Biome-BGC method).
25 The transpiration fluxes are divided between layers ($\text{TRP}_{\text{layer}}$) according to the soil moisture limitation of the
26 given layer ($\text{SMSI}_{\text{layer}}$) and the root fraction in the given layer (R_{layer} in Eq. 5):

$$27 \quad \text{TRP}_{\text{layer}} = \text{TRP}_{\text{sum}} \cdot \frac{\text{SMSI}_{\text{layer}} \cdot R_{\text{layer}}}{\text{SMSI}_{\text{sum}}} \quad (8)$$

28 where SMSI_{sum} is the sum of the $\text{SMSI}_{\text{layer}}$ values in the rootzone.

29 According to the modifications, if the soil moisture limitation is full ($\text{SMSI}=0$), no transpiration can occur.

30 4.1.6 Senescence calculation

31 The original Biome-BGC ignores plant wilting and associated senescence (where the latter is an irreversible
32 process) caused by prolonged drought. In order to solve this problem, a new module was implemented to



1 simulate the ecophysiological effect of drought stress on plant mortality. A senescence simulation has already
 2 been implemented in developed Biome-BGC (Hidy et al., 2012) and it was further improved in BBGCMuSo
 3 following a different approach. In BBGCMuSo, if the plant available SWC decreases below a critical value, the
 4 new module starts to calculate the number of the days under drought stress. Due to low SWC during a prolonged
 5 drought period, aboveground and belowground plant material senescence is occurring (actual, transfer and
 6 storage C and N pools) and the wilted biomass is translocated into the litter pool.
 7 A so-called “soil stress effect” (SSE_{total}) is defined to calculate the amount of plant material that wilts due to cell
 8 death in one day due to drought stress. The SSE_{total} quantifies the severity of the drought for a given day.
 9 Severity of drought is a function of the number of days since soil moisture stress is present (NDWS). Soil water
 10 stress is assumed if the averaged SMSI of the root zone is less than a critical value (which is an adjustable
 11 ecophysiological parameter in the model). It is assumed that after a longer time period with soil moisture stress,
 12 the senescence is complete and no living non-woody plant material remains. This longer time period is
 13 quantified by an ecophysiological parameter, which is the “critical number of stress days after which senescence
 14 mortality is complete”.
 15 The SSE_{total} varies between 0 (no stress) and 1 (total stress). According to the BBGCMuSo logic, the SSE_{total} is
 16 the function of SMSI, NDWS, $NDWS_{crit}$, and $SMSI_{crit}$:

$$SSE_{total} = SSE_{SMSI} \cdot SSE_{NDWS}$$

$$SSE_{SMSI} = \begin{cases} 1 - \frac{SMSI}{SMSI_{crit}} & ; \text{if } SMSI < SMSI_{crit} \\ 0 & ; \text{if } SMSI \geq SMSI_{crit} \end{cases} \quad (9)$$

$$SSE_{NDWS} = \begin{cases} \frac{NDWS}{NDWS_{crit}} & ; \text{if } NDWS < NDWS_{crit} \\ 1 & ; \text{if } NDWS \geq NDWS_{crit} \end{cases}$$

18 The SEE_{total} is used to calculate the actual value of non-woody aboveground and belowground mortality defined
 19 by SMCA and SMCB, respectively. SMCA defines the fraction of living C and N that dies in one day within
 20 leaves and herbaceous stems. SMCB does the same for fine roots. SMCA and SMCB are calculated using two
 21 additional ecophysiological parameters: minimum mortality coefficient (minSMC) of non-woody aboveground
 22 (A) and belowground (B) plant material senescence (minSMCA and minSMCB, respectively):

$$\begin{aligned} SMCA &= \min SMCA + (1 - \min SMCA) \cdot SSE_{total} \\ SMCB &= \min SMCB + (1 - \min SMCB) \cdot SSE_{total} \end{aligned} \quad (10)$$

24 Parameters minSMCA and minSMCB can vary between 0 and 1. In case of 0, no senescence occurs. In case of
 25 1, all living C and N will die within one day after the occurrence of drought stress. In this sense SMCA and
 26 SMCB can vary between their minimum value (minSMCA and minSMCB, respectively, if SSE_{total} is zero) and 1
 27 (if SSE_{total} is 1). This latter case occurs when $NDWS > NDWS_{crit}$ and $SMSI = 1$.
 28 SMCA is used to calculate the amount of non-woody aboveground plant material (leaves and soft stem)
 29 transferred to the standing dead biomass pool (STDB; $kgC\ m^{-2}$) due to soil moisture stress related mortality on a
 30 given day. Note that STDB is a temporary pool from which C and N contents transfer to the litter pool gradually;
 31 the concept of STDB is a novel feature in the model. In case of belowground mortality, it defines the amount of



1 fine root that goes to the litter pool directly. The actual senescence ratio is calculated as SMCA (and SMCB)
 2 multiplied with the actual living C and N pool.
 3 Fig. 3 demonstrates the senescence calculation with an example. The figure shows the connections between the
 4 change of SWC, normalized soil water content, SMSI, different types of soil stress effects (SSE_{SMSI} , SSE_{NDWS} ,
 5 SSE_{total}) and senescence mortality coefficient as function of number of days since water stress is present. The
 6 figure shows a theoretical situation in which SWC decreases from field capacity to hygroscopic water within 30
 7 days. The calculation refers to a sandy soil ($SWC_{sat} = 0.44 \text{ m}^3 \text{ m}^{-3}$, $SWC_{fc} = 0.25 \text{ m}^3 \text{ m}^{-3}$, $SWC_{wp} = 0.09 \text{ m}^3 \text{ m}^{-3}$;
 8 SWC_{fc} refers to SWC at field capacity). In this example, we assumed that that $relSWC_{crit1}$ is 1.0 (field capacity)
 9 and $relSWC_{crit2} = 0.9$ (10% below saturation), the critical number of stress days after which senescence mortality
 10 is complete ($NDWS_{crit}$) is 30 and the critical soil moisture stress index ($SMSI_{crit}$) is 0.3.

11 4.1.7 Decomposition and respiration processes

12 Within Biome-BGC, decomposition processes of litter and soil organic matter are influenced by soil
 13 temperature, soil water status, soil and litter C and N content, while root maintenance respiration is affected by
 14 soil temperature and root C and N content. In BBGCMuSo, the soil moisture and temperature limitation effects
 15 are calculated layer by layer based on the SWC and soil temperature of the given soil layer (instead of the
 16 averaged soil water status or soil temperature of the whole soil column as in the original model). The C and N
 17 contents are also calculated layer by layer from the total C and N content of the soil column weighted by the
 18 proportion of the total root mass in the given layer.

19 The maintenance root respiration flux is calculated based on the following equation:

$$20 \quad MR(\text{root}) = \sum_{\text{layer}=1}^{nr} \left(N_{\text{root}} \cdot R_{\text{layer}} \cdot mrpern \cdot Q_{10}^{\frac{T(\text{soil})_{\text{layer}} - 20}{10}} \right) \quad (11)$$

21 where n_r is the number of the soil layers which contain root, N_{root} is the total N content of the soil, R_{layer} is the
 22 proportion of the total root mass in the given layer, $mrpern$ is an adjustable ecophysiological parameter
 23 (maintenance respiration per kg of tissue N), Q_{10} is the fractional change in respiration with a 10°C temperature
 24 change and $T(\text{soil})_{\text{layer}}$ is the soil temperature of the given layer.

25 There are eight types of non-N limited fluxes between litter and soil compartments. These fluxes are the function
 26 of soil and litter C or N content, soil moisture and soil temperature stress functions. The most important
 27 innovation is that total decomposition fluxes are calculated as the sum of partial fluxes regarding to the given
 28 layer similarly to respiration flux. The soil temperature function is the same as in the original Biome-BGC. The
 29 soil moisture stress function is a linear function of SWC in contrast to a logarithmic function of soil water
 30 potential in the original Biome-BGC. A major development here is that beside drought effect, anoxic stress is
 31 also taken into account because anoxic condition caused by saturation can affect decomposition of soil organic
 32 matter (thus N mineralization; Bond-Lamberty et al., 2007). The shape of the modified stress index ($SMSI_{\text{decomp}}$)
 33 is similar to the one presented in Bond-Lamberty et al. (2007).

34 BBGCMuSo uses the following stress index (with value between 0 and 1) to control decomposition in response
 35 to changing SWC in a given layer:



$$\begin{aligned}
 \text{SMSI}_{\text{decomp}} &= \frac{\text{SWC} - \text{SWC}_{\text{hyg}}}{\text{SWC}_{\text{opt}} - \text{SWC}_{\text{hyg}}}, \text{ if } \text{SWC} \leq \text{SWC}_{\text{opt}} \\
 \text{SMSI}_{\text{decomp}} &= \frac{\text{SWC}_{\text{sat}} - \text{SWC}}{\text{SWC}_{\text{sat}} - \text{SWC}_{\text{opt}}}, \text{ if } \text{SWC}_{\text{opt}} < \text{SWC}
 \end{aligned}
 \tag{12}$$

2 where SWC, SWC_{hyg} and SWC_{sat} is the actual soil water content, hygroscopic water and the saturation values of
 3 the given soil layer, respectively. SWC_{opt} is calculated from the relative SWC for soil moisture limitation which
 4 is a user supplied ecophysiological input parameter. The limitation function of decomposition in the original
 5 Biome-BGC (based on PSI) and in BBGCMuSo (based on SWC) are presented in Fig. 4.

6 In case of the original model soil stress index starts to increase at -10 MPa (this value is fixed in the model) and
 7 reaches its maximum at saturation. In the case of BBGCMuSo, soil stress index starts to increase at hygroscopic
 8 water and reaches its maximum at optimal SWC (which is equal to the NSWC_{crit2} from Eq. 7). The new feature
 9 of BBGCMuSo is that after the optimal soil moisture content, soil stress index can decrease due to saturation soil
 10 stress (anoxic soil).

11 4.2 Management modules

12 The original Biome-BGC was developed to simulate natural ecosystems with very limited options to disturbance
 13 or human intervention (fire effect is an exception). Lack of management options limited the applicability of
 14 Biome-BGC in croplands and grasslands, but also in managed forests.

15 One major feature of BBGCMuSo is the implementation of several management options. For grasslands, grazing
 16 and mowing modules were already published as part of the developed Biome-BGC (Hidy et al., 2012).

17 Since the release of the developed Biome-BGC, we improved the model's ability to simulate management. In
 18 BBGCMuSo, the user can define 7 different events for each management activity, and additionally annually
 19 varying management activities can be defined. Further technical information about using annually varying
 20 management activities is detailed in Section 3.2. of the User's Guide (Hidy et al., 2015). Additionally, new
 21 management modules were implemented and the existing modules were further developed and extended. The
 22 detailed description of mowing and grazing can be found in Hidy et al. (2012).

23 4.2.1 Harvest

24 In arable crops, the effect of harvest is similar to the effect of mowing in grasslands but the fate of the cut-down
 25 fraction of aboveground biomass is different. We assume that after harvest, snags (stubble) remain on the field as
 26 part of the accumulated biomass, and part of the plant residue may be left on the field (in the form of litter
 27 typically to improve soil quality). Yield is always transported away from the field, while stem and leaves may be
 28 transported away (and utilized e.g. as animal bedding) or may be left at the site. The ratio of harvested
 29 aboveground biomass that is taken away from the field (harvest index) has to be defined as an input.

30 If residue is left at the site after harvest, the cut-down plant material first goes into a temporary pool that
 31 gradually enters the litter pool. The turnover rate of mown/harvested biomass to litter can be set as an
 32 ecophysiological parameter. Although harvest is not possible outside the growing season, this temporary pool
 33 can contain plant material also in the dormant period (depending on the amount of the cut-down material and the



1 turnover rate of the pool). The plant material turning into litter compartment is divided between the different
2 types of litter pools according to the parameterization (based on unstable, cellulose and lignin fractions). The
3 water stored in the canopy of the cut-down fraction is assumed to be evaporated.

4 **4.2.2 Ploughing**

5 As a management practise, ploughing may be carried out in preparation for sowing or following harvest. Three
6 types of ploughing can be defined in BBGCMuSo: shallow, medium and deep (first; first and second; first,
7 second and third soil layers are affected, respectively). Ploughing affects the predefined soil texture as it
8 homogenizes the soil (in terms of texture, temperature and moisture content) for the depth of the ploughing. We
9 assume that due to the plough the snag or stubble turns into a temporary ploughing pool on the same day. A
10 fixed proportion of the temporary ploughing pool (an ecophysiological parameter) enters the litter pool on a
11 given day after ploughing. The plant material turning into the litter compartment is divided between the different
12 types of litter pools (labile, unshielded cellulose, shielded cellulose and lignin).

13 A new feature of Biome-BBGCMuSo is that aboveground and belowground (buried) litter is handled separately in
14 order to support future applications of the model in cropland related simulations (presence of crop residues at the
15 surface affects runoff and soil evaporation). As a consequence of litterfall during the growing season and the
16 result of harvest, litter accumulates at the surface. In case of ploughing the content of aboveground litter turns
17 into the belowground litter pool. In this way aboveground/belowground litter amount can be quantified.

18 **4.2.3 Fertilization**

19 The most important effect of fertilization in BBGCMuSo is the increase of mineralized soil nitrogen. We define
20 an actual pool which contains the amount of fertilizer's nitrogen content put out onto the ground on a given
21 fertilizing day (actual pool of fertilizer; APF). A fixed proportion of the fertilizer enters the top soil layer on a
22 given day after fertilizing. It is not the entire fraction that enters the soil because a given proportion is leached
23 (this is determined by the efficiency of utilization that can be set as input parameter). Nitrate content of the
24 fertilizer (that has to be set by the user) can be taken up by the plant directly; therefore we assume that it goes
25 into the soil mineral N pool. Ammonium content of the fertilizer (that also has to be set by the user) has to be
26 nitrified before being taken up by plant, therefore it turns into the litter nitrogen pool. C content of fertilizer turns
27 into the litter C pool. As a result, APF decreases day-by-day after fertilizing until it becomes empty, which
28 means that the effect of the fertilization ends (in terms of N input to the ecosystem).

29 **4.2.4 Planting**

30 In BBGCMuSo transfer pools are defined to contain plant material as germ (or bud, or non-structural
31 carbohydrate) in the dormant season from which C and N gets to the normal pools (leaf, stem, and root) in the
32 beginning of the subsequent growing season. In order to simulate the effect of sowing we assume that the plant
33 material which is in the planted seed goes into the transfer pools thus increasing its content. Allocation of leaf,
34 stem and root from seed is calculated based on allocation parameters in the ecophysiological input data. We
35 assume that a given part of the seed is destroyed before sprouting (this can be adjusted by the user).



1 **4.2.5 Thinning**

2 Forest thinning is a new management option in BBGCMuSo. We assume that based on a thinning rate (the
3 proportion of the removed trees), the decrease of leaf, stem and root biomass pools can be determined. After
4 thinning, the cut-down fraction of the aboveground biomass can be taken away or can be left at the site. The rate
5 of transported stem and/or leaf biomass can be set by the user. The transported plant material is excluded from
6 further calculations. The plant material translocated into coarse woody debris (CWD) or litter compartments are
7 divided between the different types of litter pools according to parameterization (coarse root and stem biomass
8 go into the CWD pool; if harvested stem biomass is taken away from the site, only coarse root biomass goes to
9 CWD). Note that storage and transfer pools of woody harvested material are translocated into the litter pool.
10 The handling of the cut down, non-removed pools differs for stem, root and leaf biomass. Stem biomass (live
11 and deadwood; see Thornton, 2000 for definition of deadwood in case of Biome-BGC) is immediately
12 translocated into CWD without any delay. However, for stump and leaf biomass implementation, an intermediate
13 turnover process was necessary to avoid C and N balance errors caused by sudden changes between specific
14 pools. The parameter “Turnover rate of cut-down non-removed non-woody biomass to litter” (ecophysiological
15 input parameter) controls the fate of (previously living) leaves on cut down trees, and it also controls the
16 turnover rate of dead coarse root (stump) into CWD.

17 **4.2.6 Irrigation**

18 In case of the novel irrigation implementation we assume that the sprinkled water reaches the plant and the soil
19 similarly to precipitation. Depending on the amount of the water reaching the soil (canopy water interception is
20 also considered) and the soil type, the water can flow away by surface runoff process while the rest infiltrates
21 into the top soil layer. Irrigation amount and timing can be set by the user.

22 **4.2.7 Management related plant mortality**

23 In case of mowing, grazing, harvest and thinning, the main effect of the management activity is the decrease of
24 the aboveground plant material. It can be hypothesized that due to the disturbance related mortality of the
25 aboveground plant material, the belowground living plant material also decreases but at a lower (and hardly
26 measurable) rate. Therefore, in BBGCMuSo we included an option to simulate the decrease of the belowground
27 plant material due to management that affects aboveground biomass. The rate of the belowground decrease to the
28 mortality rate of the aboveground plant material can be set by the user. As an example, if this parameter is set to
29 0.1, the mortality rate of the belowground plant material is 10% of the mortality of the aboveground material on
30 a given management day. Aboveground material refers to actual pool of leaf, stem and fruit biomass while
31 belowground material refers to actual pool of root biomass and all the storage-transfer pools.

32 **4.3 Other plant related model processes**

33 The original Biome-BGC had a number of static features that limited its applicability in some simulations. In
34 Biome-BGC we added new features that can support model applications in a wider context, e.g. in climate



1 change related studies, modelling exercises comparing free air CO₂ enrichment (FACE) experiment data with
2 simulations (Franks et al., 2013)

3 **4.3.1 Phenology**

4 To determine the start and end of the growing season, the phenological state simulated by the model can be used
5 (White et al., 1999). We have enhanced the phenology module of the original Biome-BGC keeping the original
6 logic and providing the new method as an alternative. We developed a special growing season index (heat sum
7 growing season index; HSGSI), which is the extension of the GSI index introduced by Jolly et al. (2005). More
8 details about HSGSI can be found in Hidy et al. (2012).

9 In the original, as well as in the modified Biome-BGC model versions, snow cover did not affect the start of the
10 vegetation period and photosynthesis. We implemented a new, dual snow cover limitation method in
11 BBGCMuSo. First, the growing season can only start if the snowpack is less than a critical amount (given as mm
12 of water content stored in the snowpack). Second, the same critical value can also limit photosynthesis during the
13 growing season (no C uptake is possible above the critical snow cover; we simply assume that in case of low
14 vegetation, no radiation reaches the surface if snow depth is above a pre-defined threshold). The snow cover
15 estimation is based on precipitation, mean temperature and incoming shortwave radiation (original model logic is
16 used here). The critical amount of snow can be defined by the user.

17 **4.3.2 Genetically programmed leaf senescence**

18 Besides drought stress related leaf senescence, an optional secondary leaf senescence algorithm was
19 implemented in BBGCMuSo. For certain crops (e.g. maize and wheat), leaf senescence is the genetically
20 programmed final stage of leaf development as it is related to the age of the plant tissue in leaves. In crop
21 models, this process is traditionally determined based on the growing degree-day (GDD) sum. GDD sum is a
22 measure of heat accumulation to predict plant development stages such as flowering as well as the beginning and
23 end of grain filling. GDD is calculated using the cumulative difference between mean daily temperature and base
24 temperature (the latter is an ecophysiological input parameter in BBGCMuSo). In case of planting (i.e., in crop
25 related simulations), GDD is calculated from the day of planting. In other cases, GDD is calculated from the
26 beginning of the year. After reaching the predefined GDD threshold leaf mortality rates are calculated based on a
27 mortality coefficient of genetically programmed leaf senescence (ecophysiological input parameter).

28 **4.3.3 New plant pools: fruit and soft stem simulation**

29 In order to enable C and N budget simulation of croplands and explicit yield estimation with BBGCMuSo, fruit
30 simulation was implemented (which is grain in the case of croplands). Start of the fruit allocation is estimated
31 based on GDD. After reaching a predefined GDD value (supplied by the user as an input parameter), fruit starts
32 to grow (allocation is modified). Besides critical GDD there are four additional ecophysiological parameters that
33 have to be defined by the user related to allocation, C:N ratio of fruit, and labile and cellulose proportion of litter.
34 In order to support C and N budget simulation of non-woody biomass in BBGCMuSo, a soft stem simulation
35 was implemented (soft stem is non-photosynthesizing, aboveground, non-woody biomass). Soft stem allocation
36 is parallel to fine root and leaf allocation (and fruit allocation, if applicable). Four additional ecophysiological



1 parameters are defined due to soft stem simulation. The primary purpose of our soft stem implementation is to
 2 decrease the overestimation of LAI in herbaceous vegetation calculations. In the original model structure, in the
 3 case of herbaceous vegetation, all aboveground plant material is allocated to leaves, which causes unrealistically
 4 high LAI in many cases. Soft stem allocation (a significant pool in e.g. grasses and crops) enables more realistic
 5 leaf C and LAI values.

6 4.3.4 New C₄ photosynthesis routine

7 In the original and modified Biome-BGC models, C₄ photosynthesis was expressed as a sub-version of C₃
 8 photosynthesis. It was implemented in a way that only one parameter differed (photons absorbed by
 9 transmembrane protein complex per electron transported; mol mol⁻¹) for C₃ and C₄ plants (Collatz et al., 1991).
 10 Based on the work of Di Vittorio et al. (2010), we implemented a new, enzyme-driven C₄ photosynthesis routine
 11 into the photosynthesis module. A new ecophysiological parameter (fraction of leaf N in PEP Carboxylase) was
 12 defined in BBGCMuSo to support the C₄ routine. The ecophysiological parameter "fraction of leaf N in
 13 Rubisco" still affects the process of C₄ photosynthesis (see Di Vittorio et al., 2010 for details).

14 4.3.5 Dynamic response and temperature acclimation of respiration

15 Due to the changing environmental conditions, photosynthesis and respiration acclimation and dynamic response
 16 of plants could affect the carbon exchange rates, but this mechanism is missing from many biogeochemical
 17 models (Smith and Dukes, 2012).

18 In order to implement acclimation and short term temperature dependence of maintenance respiration in
 19 BBGCMuSo, the respiration module was modified in two steps. The maintenance respiration in Biome-BGC is
 20 based on a constant Q₁₀ factor. In our approach, first the constant Q₁₀ value was modified based on Tjoelker et al.
 21 (2001) who proposed an equation for the short-term temperature dependence of the Q₁₀ factor (dynamic
 22 response), and showed how this relationship could improve the accuracy of the modeled respiration. We use the
 23 following equation:

$$24 \quad Q_{10} = 3.22 - 0.046 * T_{\text{air}}, \quad (13)$$

25 where T_{air} is the daily average air temperature (°C).

26 This modification results in a temperature optimum at which respiration peaks. The main influence of using a
 27 temperature-dependent Q₁₀ value can be detected at high temperature values. In case of a constant Q₁₀,
 28 overestimation of respiration can occur at higher temperatures (Lombardozzi et al., 2015).

29 The model of Tjoelker et al. (2001) is a more realistic method to calculate respiration but it does not take into
 30 account acclimation to the longer term changes in thermal conditions.

31 Long-term responses of respiration rates to the temperature (i.e., acclimation) were implemented in the second
 32 step based on Atkin et al. (2008) who developed a method using the relationship between leaf respiration, leaf
 33 mass-to-area ratio, and leaf nitrogen content in 19 species of plants grown at four different temperatures. The
 34 proposed equation is the following:

$$35 \quad R_A = R_T * 10^{A * (T_{0\text{days}} - T_{\text{ref}})}, \quad (14)$$



1 where R_T is the non-acclimated rate of respiration, T_{ref} is the reference temperature, T_{10days} is the average daily
 2 temperature in the preceding 10 days, and A is a constant, which was set to 0.0079 based on Atkin et al. (2008).
 3 The acclimated and non-acclimated day and night leaf maintenance respiration functions are presented in Fig. 5.
 4 Photosynthesis acclimation is in a test phase. It is simulated in a very simple way by modifying the relationship
 5 between V_{cmax} (maximum rate of carboxylation) and J_{max} (maximum electron transport rate) that was
 6 temperature-independent in the original code. Temperature dependency is calculated based on average
 7 temperature for the previous 30 days (Knorr and Kattge, 2005). This simple photosynthesis method is not a
 8 complete representation of the acclimation of the photosynthetic machinery (Smith and Dukes, 2012) but a first
 9 step towards a more complete implementation. This feature can be enabled or disabled by the user.

10 4.3.6 LAI-dependent albedo

11 In order to improve the shortwave radiative flux estimation of BBGCMuSo, an LAI-dependent albedo estimation
 12 was implemented based on the method of Ritchie (1998). Actual albedo is calculated by the following equation:

$$13 \alpha_{act} = \alpha_{crit} - (\alpha_{crit} - \alpha_{BS}) \cdot \exp(-0.75 \cdot LAI_{act}), \quad (15)$$

14 where α_{crit} is an empirical estimate of the albedo maximum (0.23), α_{BS} is the albedo of the bare soil that has to be
 15 supplied by the user, and LAI_{act} is the actual value of leaf area index as estimated by the model.

16 4.3.7 Stomatal conductance regulation

17 Although there are many alternative formulations for stomatal conductance calculation within biogeochemical
 18 models (e.g., Damour et al., 2010), there is no standard method in the scientific community. Many state-of-the-
 19 art ESMs use a variant of the Ball-Woodrow-Berry model (Ball et al., 1987), the Leuning (1995) method, and
 20 the Jarvis (1976) method. There is no proof that one method is significantly better than the other (Damour et al.,
 21 2010).

22 Traditionally, Biome-BGC uses the empirical, multiplicative Jarvis method for stomatal conductance
 23 calculations (Jarvis, 1976). In this method, stomatal conductance is calculated as the product of the maximum
 24 stomatal conductance (model parameter) and limiting stress functions based on minimum temperature, VPD, and
 25 soil water status (Trusilova et al., 2009).

26 In BBGCMuSo, we kept this logic as its applicability was demonstrated in many studies (see Introduction). In
 27 contrast to the original model, the stress function of soil water status is currently based on relative soil water
 28 content and the introduced SMSI (instead of soil water potential) (Hidy et al., 2012). Beyond this, we modified
 29 the original method of calculation to take into account the changes in ambient CO_2 concentration. It was
 30 demonstrated that the stomatal response of Biome-BGC to increasing atmospheric CO_2 concentration is not
 31 consistent with observations (Sándor et al., 2015; note the latter study used BBGCMuSo 2.2 for which the
 32 modification was not yet implemented). Therefore, we implemented an additional multiplicative factor in the
 33 calculations in BBGCMuSo 4.0.

34 In Biome-BGC, stomatal conductance is the function of maximum stomatal conductance (that is an input
 35 ecophysiological parameter) and a set of limitation factors. These multiplicative limitation factors summarize the
 36 effects of SWC, minimum soil temperature, VPD and photosynthetic photon flux density. As we mentioned



1 above (Section 3.2.1), we modified the limitation function of SWC on stomatal conductance. Besides this
 2 modification, a new CO₂ concentration dependent adjustment factor was implemented in order to improve
 3 stomatal calculation based on Franks et al. (2013). They demonstrated a significantly similar dependence of
 4 stomatal conductance on ambient CO₂ concentration from hourly to geological time scales. Though the Franks et
 5 al. (2013) paper presents results for stomatal conductance in general (as opposed to maximum stomatal
 6 conductance), we use the assumption that the same function describes changes in maximum stomatal
 7 conductance as well. This assumption is acceptable since stomatal conductance has an upper limit which is
 8 present in conditions without environmental stress and with maximum illumination.

9 In our approach, data from Franks et al. (2013; Table S1) was used to fit a power function to describe the
 10 quantitative relationship between relative change of stomatal conductance ($g_{w(\text{rel})}$; in fact this is stomatal
 11 conductance to water vapour but this is proportional to stomatal conductance to CO₂) to changes of ambient CO₂
 12 mixing ratio (Fig. 7b in Franks et al., 2013). The changes are expressed relative to standard conditions:

$$13 \quad g_{w(\text{rel})} = 39.43 \cdot [\text{CO}_2]^{-0.64} \quad (16)$$

14 where [CO₂] is atmospheric CO₂ mixing ratio in ppm. In BBGCMuSo v4.0, maximum stomatal conductance is
 15 first re-calculated according to the actual CO₂ concentration (this latter is supplied by the user for each
 16 simulation year). As maximum stomatal conductance is no longer constant (which was the case in the original
 17 Biome-BGC and also in BBGCMuSo up to version 3.0), it is assumed that the maximum stomatal conductance
 18 defined by the user represents end of the 20th century conditions (at ~360 ppm mixing ratio representing ~ year
 19 1995 conditions; $g_{\text{smax_EPC}}$).

20 To calculate actual maximum stomatal conductance, first $g_{w(\text{rel})}$ is calculated at 360 ppm according to Eq. 13
 21 ($g_{w(\text{rel})|360\text{ppm}} = 39.43 \cdot 360^{-0.64} = 0.9116$; note that this value is not exactly one because of the scatter of data used to
 22 fit the power function). Next, $g_{w(\text{rel})}$ is calculated for the given [CO₂] value according to Eq. 16. The final
 23 maximum stomatal conductance (g_{smax}) is calculated as:

$$24 \quad g_{\text{smax}} = g_{w(\text{rel})} / 0.9116 \cdot g_{\text{smax_EPC}} \quad (17)$$

25 The final maximum stomatal conductance is used for subsequent calculations for evapotranspiration and
 26 photosynthesis. This modification is essential for climate-change related simulations.

27 **4.4 Modification in the model run**

28 **4.4.1 Dynamic mortality**

29 Annual whole-plant mortality fraction (WPM) is part of the ecophysiological parameterization of Biome-BGC
 30 (user supplied value) which is assumed to be constant throughout the simulation. From the point of view of
 31 forest growth, constant mortality can be considered as a rough assumption. Ecological knowledge suggests that
 32 WPM varies dynamically within the lifecycle of forest stands due to competition for resources or due to
 33 competition within tree species (plus many other causes; Hlásny et al., 2014).

34 In order to enable more realistic forest stand development simulation, we implemented an option for supplying
 35 annually varying WPM to BBGCMuSo (this option can also be used with other biome types with known,
 36 annually varying disturbance level). During the normal phase of the simulation, the model can either use



1 constant mortality or it can use annually varying WPM defined by the user. Technical details about the
2 application of this option can be found in Section 3.6 of the BBGCMuSo v4.0 User's Guide (Hidy et al., 2015).

3 **4.4.2 Optional transient run**

4 Model spinup in Biome-BGC typically represents steady-state conditions before the industrial revolution
5 (without changing atmospheric CO₂ concentration and N deposition). Therefore, the usual strategy for spinup is
6 to use constant (preindustrial) CO₂ and N_{dep} values during the spinup followed by annually varying values for the
7 entire normal simulation (representative to present day conditions or to 20th century conditions). This strategy
8 might be used due to unknown site history or a lack of driving data. However, this logic can lead to undesired
9 transient behavior of the model results as the user may introduce a sharp change by the inconsistent CO₂ and/or
10 N_{dep} data between the spinup and normal phase (note that both CO₂ and N_{dep} are important drivers of plant
11 growth).

12 In order to avoid this phenomena (and more importantly, to take into account site history), some model users
13 performed one or more transient simulations to enable smooth transition from one simulation phase to the other
14 (mainly, from the spinup phase to the normal phase; Thornton et al., 2002; Vetter et al., 2005; Hlásny et al.,
15 2014). However, this procedure means that the users have to perform a 3rd model run (and sometimes even
16 more), using the output of the spinup phase, and create the input that the normal phase can use.

17 In BBGCMuSo, we implemented a novel approach to eliminate the effect of sharp changes in the environmental
18 conditions between the spinup and normal phase. According to the modifications, now it is possible to make an
19 automatic transient simulation after the spinup phase.

20 To initiate the transient run, the user can adjust the settings of the spinup run. If needed, a regular spinup will
21 first be performed with constant CO₂ and N deposition values followed by a second run to be performed using
22 the same meteorological time series defined for the spinup. In this way, the length of the transient run is always
23 equal to the length of the meteorology data used for the spinup phase. During the transient run, annually varying
24 CO₂ concentration data can be used (but it should be constructed to provide transition from preindustrial to
25 industrial CO₂ concentrations). Utilization of annually varying N-deposition data is optional but it is preferred.
26 The input data of transient run is the output of the spinup phase, and the output of the transition run is the input
27 of the normal phase. Technical details about the transient run can be found in Section 2.2 of the User's Guide
28 (Hidy et al., 2015).

29 As management might play an important role in site history (and consequently in biogeochemical cycles), the
30 new transient simulation in BBGCMuSo can include management in an annually varying fashion (management
31 is described below).

32 **4.4.3 Land-use-change simulations**

33 Another new feature was added to BBGCMuSo that is also related with the proper simulation of site history. As
34 the spinup phase is usually associated with preindustrial conditions, the normal phase might represent a plant
35 functional type that is different from the one present in the spinup phase. For example, present-day croplands can
36 occupy land that was originally forest or grassland, so in this case spinup will simulate forest in equilibrium, and
37 then the normal phase will simulate croplands. Another example is the simulation of afforestation that might



1 require spinup for grasslands, and normal phase for woody vegetation. We may refer to these scenarios as land
2 use change (LUC) related simulations.
3 One problem that is associated with LUC is the frequent crash of the model with the error 'negative nitrogen
4 pool' during the beginning of the normal phase. This error is typical if the spinup and normal ecophysiological
5 parameterization differ in terms of plant C:N ratios (due to the internal model logic; inconsistency might arise
6 between available mineralized N and N demand by the plant, and this might cause a negative nitrogen pool).
7 In order to avoid this error, we have implemented the following automatic procedure. According to the changes,
8 only the equilibrium C pools are passed to the normal phase after the spinup phase has ended. The equilibrium
9 nitrogen pools are calculated by the model code so that the resulting C:N ratios are harmonized with the C:N
10 ratio of the different plant compartments presented in the ecophysiological parameterization of the normal phase.
11 This modification means that equilibrium nitrogen pools are not passed to the normal phase. We believe this
12 issue is compensated with the fact that LUC and site history can be simulated properly.

13 **4.5 Empirical estimation of other greenhouse gases**

14 Quantification of the full greenhouse gas (GHG) balance of ecosystems was not possible with the original
15 Biome-BGC. Non-CO₂ greenhouse gases (GHGs) are important elements of the biogeochemistry of the soil-
16 plant system. Nitrous oxide (N₂O) and methane (CH₄) are strong GHGs that can eventually compensate the CO₂
17 sink capacity of ecosystems resulting in GHG-neutral or GHG source activity (Schulze et al., 2009). We
18 established the first steps towards improved modeling possibilities with Biome-BGC that includes soil efflux
19 estimation of non-CO₂ GHGs.

20 **4.5.1 Estimation of nitrous oxide and methane flux of unmanaged soil**

21 Due to their importance, an empirical estimation of N₂O and CH₄ emission from soils was implemented in
22 BBGCMuSo based on the method of Hashimoto et al. (2011). Gas fluxes are described in terms of three
23 functions: soil physiochemical properties (C:N ratio for N₂O; bulk density of top soil layer for CH₄), water-filled
24 pore space (WFPS) of top soil layer, and soil temperature of top soil layer.
25 The Hashimoto et al. (2011) method was developed for unmanaged ecosystems. We adapted it to managed
26 ecosystems by including emission estimates from livestock and manure management using Tier 1 methods of
27 IPCC (2006).

28 **4.5.2 Estimation of nitrous oxide and methane flux from grazing and fertilizing**

29 The IPCC (2006) Tier 1 method was implemented in BBGCMuSo to give a first estimation to CH₄ and N₂O
30 emissions due to grazing and fertilizing.
31 Due to their large population and high CH₄ emission rate, cattle are an important source of CH₄. Methane
32 emissions of cattle originate from manure management (including both dung and urine) and enteric emissions.
33 Methane emission from enteric fermentation is estimated using the number of the animals and the regional-
34 specific methane emission factor from enteric fermentation (IPCC, 2006; Chapter 10, Table 10.11). Another
35 mode of methane production is the emission during the storage of manure. Methane emission from manure



1 management is estimated using the number of animals and the regional-specific methane emission factor from
2 manure management (IPCC, 2006; Chapter 10, Table 10.14).

3 In summary, the flux of the methane (F_{CH_4} ; $\text{mg CH}_4 \text{ m}^{-2} \text{ day}^{-1}$) is the sum of soil flux, flux from fermentation and
4 from manure management:

$$5 \quad (F_{\text{CH}_4})_{\text{total}} = (F_{\text{CH}_4})_{\text{soil}} + (F_{\text{CH}_4})_{\text{fermentation}} + (F_{\text{CH}_4})_{\text{manure}} \quad (18)$$

6 The emissions of N_2O that result from anthropogenic N inputs or N mineralization occur through both direct
7 pathways (directly from the soils to/from which the N is added/released – grazing and fertilization), and through
8 indirect pathways (volatilization, biomass burning, and leaching). Volatilization fluxes were already
9 implemented into BBGCMuSo. Direct emissions of N_2O from managed soils consist of the emission from
10 animal excretion and from fertilization. The former is estimated based on multiplying the total amount of N
11 excretion by an emission factor for that type of manure management system (IPCC, 2006; Chapter 10, Table
12 10.21). The latter is estimated using emission factors developed for N_2O emissions from synthetic fertilizer and
13 organic N application (IPCC, 2006; Chapter 11, Table 10.21).

14 In summary, the flux of the nitrous oxide ($F_{\text{N}_2\text{O}}$; $\text{mg N}_2\text{O m}^{-2} \text{ day}^{-1}$) is the sum of soil flux, flux from
15 fermentation and from manure management:

$$16 \quad (F_{\text{N}_2\text{O}})_{\text{total}} = (F_{\text{N}_2\text{O}})_{\text{soil}} + (F_{\text{N}_2\text{O}})_{\text{grazing}} + (F_{\text{N}_2\text{O}})_{\text{fertilizing}} \quad (19)$$

17 5 Simulation results: model evaluations

18 In order to examine and evaluate the functioning of BBGCMuSo, case studies are presented in this section
19 regarding different vegetation types: C_3 grassland (Bugac, Hungary), C_4 maize (Mead, Nebraska, United States
20 of America) and C_3 oak forest (Jastrebarsko, Croatia).

21 The model behavior is evaluated by visual comparison of measured and simulated data and by quantitative
22 measures such as root mean squared error (RMSE), normalized root mean squared error (RMSE weighted by the
23 difference of maximum and minimum of the measured data), bias (average difference between simulated and
24 measured variables, where positive bias means systematic overestimation and negative bias means overall
25 underestimation), coefficient of determination (R^2) of the regression between measured and modeled data, and
26 Nash–Sutcliffe modeling efficiency (NSE). The range of NSE is between 1.0 (perfect fit) and $-\infty$. An efficiency
27 of lower than zero means that the mean of the observed time series would have been a better predictor than the
28 model. NSE and R^2 are dimensionless. The dimension of RMSE and bias is the dimension of the variable to
29 which it refers. The dimension of NRMSE is %.

30 In this study, model parameters were taken from the literature, and also from previous parameterization of
31 Biome-BGC. For the newly introduced parameters, we use values that provided reasonable results during model
32 development. The number of parameters in the original model (Biome-BGC v4.1.1 MPI) and BBGCMuSo
33 (Biome-BGCMuSo v4.0) is not the same (MuSo has more ecophysiological parameters than original model,
34 while a few parameters of the original model are no longer used in BBGCMuSo) but the same values were set in
35 case of common parameters.



1 The simulation results of the original Biome-BGC and BBGCMuSo are compared to the measurements.
2 Different model features such as the senescence mechanism, management, and groundwater effects are
3 illustrated in the Supplementary material (S1-S9).
4 BBGCMuSo has more than 600 different output variables. In this study, we focus on the variables relevant for
5 the evaluation of model performance: that are GPP, TER, net ecosystem exchange (NEE), LHF, LAI, C content
6 of aboveground biomass (abgC), and SWC in the 10-30 cm soil layer.
7

8 **5.1 C₃ grassland/pasture**

9 Measured data at Bugac are available from 2003 to 2015. In order to present model behavior, only three
10 consecutive years were selected (2009-2011) that represented different meteorological conditions. In 2009, the
11 annual sum of precipitations was 14% lower, and mean annual temperature was 10% higher than the long term
12 mean. In 2010, precipitation was 65% higher and temperature was near average (2% lower). In 2011,
13 precipitation was 22% lower than average and temperature was close to the long term mean.

14 For the Bugac simulation, several novel features were used from BBGCMuSo v4.0. The HSGSI-based
15 phenology, transient simulation, drought related plant senescence, standing dead biomass pool, grazing settings
16 (see Hidy et al. (2015) for grazing related input data), non-zero soft stem allocation, management-related
17 decrease of storage and the actual pool, and acclimation were all used in the simulation.

18 Both during spinup and normal phase of the simulation we assumed that the vegetation type is grassland,
19 therefore the C₃ grass parameterization was used (see Supplementary material Table S1 for parameterization).

20 Fig. 6 shows that the original Biome-BGC overestimates GPP, TER, LAI and LHF. Due to the implementation
21 of grazing and plant senescence processes, the overestimation of GPP, TER and LHF were decreased at the
22 Bugac site where drought frequently occurs. The average observed maximum LAI is about 4-5 m² m⁻² at Bugac.
23 Therefore, due to model improvements simulated LAI is more realistic using BBGCMuSo. This was possible
24 due to the implementation of the new soft stem pool that now can contain part of the aboveground C (in the
25 original model, all aboveground C formed leaf biomass for grasses).

26 The results of the quantitative model evaluation are presented in Table 3 for Bugac using the original Biome-
27 BGC and the BBGCMuSo. The statistical indicators show that with the exception of SWC, the simulation
28 quality typically improved due to the model developments. The error metrics are usually smaller, R² is higher
29 than in case of the original model using the original parameter set. BBGCMuSo-simulated LHF has higher bias
30 (in absolute sense) than the original model, but the other error metrics perform better. It is notable that NSE
31 became positive for GPP, TER and LHF while it was negative for all three variables with the original Biome-
32 BGC.

33 The SWC estimation by the original model was closer to the observations than the result with BBGCMuSo.
34 However, as the original Biome-BGC has a simple, one-layer bucket module for soil hydrology, SWC estimation
35 by the original model and topsoil SWC simulation by Biome-BGCmuSo are not comparable. SWC provided by
36 the original model has no vertical profile, which means that it is not expected that the simulation will match
37 observation. Nevertheless, although the errors are higher in case of BBGCMuSo (RMSE, NRMSE, NSE, BIAS),
38 the correlation is higher. This is relevant because in the BBGCMuSo simulation, the relative change of soil water



1 content significantly impacts the senescence and decomposition fluxes (see Section 3.2). Therefore, if the
2 relative change of the soil water content is realistic, the soil moisture limited processes can still be realistic in
3 spite of the obvious bias in the measurements.

4 Supplementary material S2 contains additional simulation results for Bugac demonstrating the effect of the long
5 lasting drought on plant state, the senescence effect on plant processes and carbon balance and the effect of
6 grazing.

7 5.2 C4 cropland

8 Measured data and simulated results are presented for the 2003-2006 period for the Mead1 site (Fig. 7).

9 For Mead, the applied novel features with BBGCMuSo included C₄ enzyme-driven photosynthesis, transient
10 simulation, planting, harvest, irrigation, drought related plant senescence, genetically programmed leaf
11 senescence, standing dead biomass pool, fruit pool (in this case maize yield), non-zero soft stem allocation, and
12 acclimation. Note that the allocation related “current growth proportion” parameter that controls the content of
13 the storage pool (non-structured carbohydrate reserve for next year’s new growth) was zeroed here in order to
14 avoid natural plant growth in the spring. In other words, in case of planting, the storage pool has to be turned off
15 as maize growth is only possible after sowing.

16 During the spinup phase, we assumed that the vegetation type was grassland before cropland establishment.
17 Therefore C₃ grass parameterization was used. In the normal phase, maize parameterization was used. Note that
18 change in ecophysiological parameterization was possible due to the developments (see Section 2).
19 Supplementary material Table S1 contains the complete parameterization for the maize simulation.

20 As noted (Section 3.5.2), there is a high chance for model error if the spinup and normal ecophysiological
21 parameterization differ in terms of plant C:N ratios (due to the internal model logic). To avoid this error, in the
22 case of original Biome-BGC, the C:N ratios of maize were used in the spinup phase. Mead1 is under
23 management including irrigation, fertilization, harvest, and ploughing. The original model assumes that the
24 vegetation is undisturbed, so no management practices could be set. For BBGCMuSo, management was set
25 according to information taken from the site PI.

26 Fig. 7 shows that the original model underestimated GPP in the vegetation period (in contrast to BBGCMuSo)
27 because it cannot take into account the effect of irrigation and fertilization, which support the growth of
28 agricultural crops. The original model overestimated GPP following harvest because plant material was not
29 removed from the site. Using BBGCMuSo, the overestimation of TER and LAI decreased compared to the
30 original model due to the simulated harvest. For BBGCMuSo this overestimation decreased also due to the novel
31 fruit and soft stem simulations (in the original model, aboveground plant material apportioned biomass to leaves
32 only).

33 The results of the quantitative model evaluation are presented in Table 4 for Mead using the original Biome-
34 BGC and the BBGCMuSo. According to the error metrics the simulation quality improved due to the model
35 developments for GPP, TER, LAI and abgC, and also for SWC. For BBGCMuSo, the errors (both RMSE and
36 bias) are smaller and square of correlations are higher than in case of the original model using the original
37 parameters. Values of NSE are close to 1.0 using BBGCMuSo indicating a good match of the modeled values
38 and the observed data. For the original model, NSE values are much smaller or negative. NSE is negative for



1 SWC both for the original and the BBGCMuSo version in spite of the lower bias of the latter. Again, due to the
2 very simplistic SWC module of the original model, its SWC results are not directly comparable with
3 observations.

4 Supplementary material S3 presents additional simulation results for the Mead1 site demonstrating the effect of
5 new model developments like irrigation fertilization, and the genetically programmed leaf senescence.

6 **5.3 Deciduous broad-leaved forest**

7 For Jastrebarsko forest site measurement data were available for the period from 2008 to 2014. But, as the
8 measurement height was changed in spring 2011 (flux tower was upgraded due to tree growth), to assure the
9 homogeneity of the measurement data we used data from 2008-2010 only.

10 For simulation at Jastrebarsko, several novel features were used from BBGCMuSo v4.0. For example, transient
11 simulation, alternative tipping bucket soil water balance calculation, groundwater effect on stomatal conductance
12 and decomposition, drought related plant senescence, thinning, fruit allocation, bulk denitrification, soil moisture
13 limitation calculation, soil stress index, soil texture change through the soil profile, and respiration acclimation
14 were all used in the simulation. We also used the possibility to adjust the parameter for maintenance respiration,
15 which is fixed within the source code in the original Biome-BGC model. We used the value of $0.4 \text{ kg C kg N}^{-1} \text{ day}^{-1}$
16 based on newly available data (Cannell and Thornley, 2000).

17 During both spinup and normal phase we assume that the vegetation type was pedunculate oak forest, therefore
18 oak parameterization was used (see Supplementary material Table S1 for parameterization).

19 Fig. 8 shows that the original Biome-BGC overestimates GPP, TER, NPP and LAI. Probable reason for this is
20 high N fixation parameter value, estimated to $0.0036 \text{ g N m}^{-2} \text{ yr}^{-1}$, resulting from the presence of N-fixer species
21 *Alnus glutinosa* (see Supplement for details) and, at the same time, the lack of denitrification process in the
22 original Biome-BGC version. Due to the implementation of dry and wet bulk denitrification processes, effects of
23 groundwater, and soil moisture stress in the BBGCMuSo version the overestimation of GPP, TER, and NPP was
24 no longer present and simulation results significantly improved. Jastrebarsko forest site is a lowland oak forest
25 with complex soil hydrology which cannot easily be simulated using simple soil bucket approach, as it is a case
26 in original Biome-BGC model. Soil at Jastrebarsko site is stagnic luvisol, with impermeable clay horizon at 2-3
27 m depth and poor vertical water conductivity, resulting with parts of the forest being partly waterlogged or even
28 flooded with stagnating water during winter and early spring. Flooding leads to increased denitrification
29 (Groffman and Tiedje, 1989; Kulkarni et al., 2014) and, in combination with hypoxic conditions in the root zone,
30 reflects negatively on GPP and TER (Fig. 8a,b).

31 Soil water content simulation in BBGCMuSo version shows improvement for the leaf-off season (Nov-Apr)
32 when, unlike the original version, soil water saturation in BBGCMuSo simulation becomes evident (Fig. 8c).
33 BBGCMuSo still overestimates soil moisture status in the summer. According to the original Biome-BGC the
34 forest never experiences soil saturation which is contrary to the actual situation in winter and early spring.
35 Original Biome-BGC provides only SWC data for one layer of the entire rooting zone (0-100 cm in this case)
36 and therefore it cannot be directly compared with the actual measurements or output from BBGCMuSo which
37 correspond to 0-30 cm soil layer. Also, it should be emphasized that the parameters soil bulk density, SWC of



1 saturation, field capacity, and wilting point for soil layers were not available. BBGCMuSo calculated those
2 parameters based only on the provided parameters for soil texture.
3 Simulated LAI value also decreased to more realistic values in BBGCMuSo due to model improvements (Fig.
4 8d). Based on litterfall data (0.408 kg m^{-2} ; Marjanović et al. (2011b)) and average specific leaf area of $15 \text{ m}^2 \text{ kg}^{-1}$
5 for oak (Morecroft and Roberts, 1999), the average maximum LAI at Jastrebarsko is estimated to be $6.1 \text{ m}^2 \text{ m}^{-2}$,
6 just slightly above what is estimated by BBGCMuSo. BBGCMuSo NPP estimates are also in good agreement
7 with those from field observation (Marjanović et al., 2011a), unlike those of the original version which
8 overestimate NPP (Fig. 8e)
9 The results of the quantitative model evaluation are presented in Table 5 for Jastrebarsko site using the original
10 Biome-BGC and the BBGCMuSo. The quality of simulation usually improved with BBGCMuSo due to the
11 model developments (R^2 for SWC is an exception, but see the notes above about the SWC simulation of the
12 original Biome-BGC). Key variables' errors and biases are smaller in comparison to the original model using the
13 original parameter set.
14 Supplementary material S4 contains additional simulation results for the Jastrebarsko site demonstrating the
15 effect of new model developments.

16 **6 Discussion and conclusions**

17 Biogeochemical models inevitably need continuous improvement to improve their ability to simulate ecosystem
18 C balance. In spite of the considerable development in our understanding of the C balance of terrestrial
19 ecosystems (Baldocchi et al., 2001; Friend et al., 2006; Williams et al., 2009), current biogeochemical models
20 still have inherent uncertainties. The major sources of uncertainties are internal variability, initial and boundary
21 conditions (e.g. equilibrium soil organic matter pool estimation), parameterization and model formulation
22 (process representation) (Schwalm et al., 2015; Sándor et al., 2016).

23 In this study, our objective was to address model structure related uncertainties in the widely used Biome-BGC
24 model.

25 The interactions between water availability and ecosystem C balance are widely documented in the literature. In
26 a recent study, Ahlström et al. (2015) showed that semi-arid ecosystems have strong contribution to the trend
27 and interannual variability of the terrestrial C sink. This finding emphasizes the need to accurately simulate soil
28 water related processes and plant senescence due to prolonged drought. In earlier model versions, drought could
29 not cause plant death (i.e., LAI decrease) which resulted in a quick recovery of the vegetation after a prolonged
30 drought. In our implementation, long lasting drought can cause irreversible plant senescence which is more
31 realistic than the original implementation.

32 Role of management as the primary driver of biomass production efficiency in terrestrial ecosystems was shown
33 by Campioli et al. (2015). The study clearly demonstrates that management cannot be neglected if proper
34 representation of the ecosystem C balance is needed. The management modules built into BBGCMuSo cover, on
35 a global basis, the majority of human interventions in managed ecosystems. As management practises require
36 prescribed input data for BBGCMuSo, accuracy of the simulations will clearly depend on the quality of
37 management description which calls for proper data to drive the model.



1 Representation of acclimation of plant respiration and photosynthesis was shown to be one major uncertainty in
2 global biogeochemical models (Lombardozi et al., 2015). We introduced acclimation of autotrophic respiration
3 in BBGCMuSo which is a major step towards more realistic climate change related simulations. Representation
4 of photosynthesis acclimation (Medlyn et al., 2002) is needed in future modifications as another major
5 development.

6 Due the implementation of many novel model features, the model logic became more complex. Thus, process
7 interactions became even more complicated which means that extensive testing is needed to find problems and
8 limitations.

9 The earlier version of BBGCMuSo (v2.2) was already used in a major model intercomparison project (FACCE
10 MACSUR – Modelling European Agriculture with Climate Change for Food Security, a FACCE JPI knowledge
11 hub; Ma et al., 2014; Sándor et al., 2016). Within MACSUR, nine grassland models were used and their
12 performance was tested against EC and biomass measurements. BBGCMuSo v2.2 results were comparable with
13 other models like LPJmL, CARAIB, STICS, EPIC, PaSim, and others. In spite of the successful application of
14 the predecessor of BBGCMuSo v4.0, SWC simulations were still problematic (Sándor et al., 2016).
15 Developments are clearly needed in terms of soil water balance and ecosystem scale hydrology in general.

16 Other developments are still needed to improve simulations with dynamic C and N allocation within the plant
17 compartments (Friedlingstein et al., 1999; Olin et al., 2015). Complete representation of ammonium and nitrate
18 pools with associated nitrification and denitrification is also needed to avoid ill-defined, N balance related
19 parameters (Thomas et al., 2013).

20 In the present paper three case studies were presented to demonstrate the effect of model structural
21 improvements on the simulation quality. Clearly, extensive testing is required at multiple EC sites to evaluate the
22 performance of the model and to make adjustments if needed.

23 Parameter uncertainty also needs further investigations. Model parameterization based on observed plant traits is
24 possible today thanks to new datasets (e.g., White et al., 2000; Kattge et al., 2011; van Bodegom et al., 2012).
25 However, in some cases, imperfect model structure may cause distortion owing to compensation of errors
26 (Martre et al., 2015). Additionally, plant traits (e.g. specific leaf area, leaf C:N ratio, photosynthesis-related
27 parameters) vary considerably in space so even though plant trait datasets are available they might not capture
28 the site-level parameters. These issues raise the need for proper infrastructure for parameter estimation (or in
29 other words, calibration or model inversion). The need for model calibration is also emphasized as we introduced
30 a couple of empirical parameters in BBGCMuSo (e.g. those related to plant senescence, water stress thresholds
31 and denitrification drivers, disturbance-related mortality parameters) that need optimization using measurement
32 data from multiple sites. In other words, though BBGCMuSo parameterization is mostly based on observable
33 plant traits, model calibration can not be avoided in the majority of the cases (Hidy et al., 2012).

34 To address this problem we created a computer-based open infrastructure that can help a wide array of users in
35 the application of the new model. We followed the concept of model-data fusion (MDF; Williams et al., 2009)
36 when developing the so-called “Biome-BGC Projects Database and Management System” (BBGCDB;
37 <http://ecos.okologia.mta.hu/bbgcdb/>) and the BioVeL Portal (<http://portal.biovel.eu>) as a virtual research
38 environment and collaborative tool. BBGCDB and the BioVeL portal help parameter optimization of
39 BBGCMuSo by a computer cluster-based Monte Carlo experiment and GLUE methodology (Beven and Binley,



1 1992). Further integration is planned using an alternative a Bayesian calibration algorithms (Hartig et al., 2012),
2 that will provide extended calibration options to the parameters of BBGCMuSo.
3 We would like to support BBGCMuSo application for the wider scientific community as much as possible. For
4 users of the original Biome-BGC, the question is of course the following: should I move to BBGCMuSo? Does
5 it need a long learning process to move to the improved model? We would like to stress that users of the original
6 Biome-BGC will have a smooth transition to BBGCMuSo, as we mainly preserved the structure of the input
7 files. The majority of changes are related to the 7-layer soil module and to the implementation of management
8 modules. The ecophysiological parameter file is similar to the original but it was extended considerably. This
9 may raise issues but as it is emphasized in our User's Guide (Hidy et al., 2015), we extended the
10 ecophysiological parameter file with many parameters that will not need adjustment in the majority of the cases.
11 We simply moved some 'burned-in' parameters into the ecophysiological parameter in order to allow easy
12 adjustment if needed in the future.

13 **Code availability**

14 The source code, the Windows model executable, sample simulation input files and documentation are available
15 at the BBGCMuSo website (<http://nimbus.elte.hu/bbgc>).

16 **Authors' Contributions**

17 Hidy developed Biome-BGCMuSo with modifying Biome-BGC 4.1.1 MPI version. The study was conceived
18 and designed by Hidy and Barcza, with assistance from Marjanović, Churkina, Fodor, Horváth, and Running. It
19 was directed by Barcza and Hidy. Marjanović, Ostrogović Sever, Pintér, Nagy, Gelybó, Dobor and Suyker
20 contributed with simulations, measurement data and its post-processing and ideas on interpretation of the model
21 validation. Hidy, Barcza and Marjanović prepared the manuscript and the supplement with contributions from all
22 co-authors. All authors reviewed and approved the present article and the supplement.
23



1 **Acknowledgements**

2 The research was funded by the Hungarian Academy of Sciences (MTA PD 450012), the Hungarian Scientific
3 Research Fund (OTKA K104816), the BioVeL project (Biodiversity Virtual e-Laboratory Project, FP7-
4 INFRASTRUCTURES-2011-2, project number 283359), the EU FP7 WHEALBI Project (Wheat and Barley
5 Legacy for Breeding Improvement; project No. 613556), the Croatian Science Foundation Installation Research
6 Project EFFEffectivity (HRZZ-UIP-11-2013-2492), and metaprogramme Adaptation of Agriculture and Forests to
7 Climate Change (AAFCC) of the French National Institute for Agricultural Research (INRA). We acknowledge
8 the international research project titled “FACCE MACSUR – Modelling European Agriculture with Climate
9 Change for Food Security, a FACCE JPI knowledge hub”. Biome-BGC version 4.1.1 (the predecessor of
10 BBGCMuSo) was provided by the Numerical Terradynamic Simulation Group (NTSG) at the University of
11 Montana, Missoula MT (USA), which assumes no responsibility for the proper use by others. We are grateful to
12 the Laboratory of Parallel and Distributed Systems, Institute for Computer Science and Control (MTA SZTAKI),
13 that provided consultation, technical expertise and access to the EDGeS@home volunteer desk top grid system
14 in computationally demanding analysis.
15



1 **References**

- 2 Ahlström, A., Raupach, M. R., Schurgers, G., Smith, B., Arneeth, A., Jung, M., Reichstein, M., Canadell, J. G.,
 3 Friedlingstein, P., Jain, A. K., Kato, E., Poulter, B., Sitch, S., Stocker, B. D., Viovy, N., Wang, Y. P., Wiltshire,
 4 A., Zaehle, S. and Zeng, N.: The dominant role of semi-arid ecosystems in the trend and variability of the land
 5 CO₂ sink, *Science*, 348, 895–899, doi:10.1126/science.aaa1668, 2015.
- 6 Alberti, G., Vicca, S., Inghima, I., Beilelli-Marchesini, L., Genesio, L., Miglietta, F., Marjanovic, H., Martinez,
 7 C., Matteucci, G., D'Andrea, E., Peressotti, A., Petrella, F., Rodeghiero, M. and Cotrufo, M. F.: Soil C:N
 8 stoichiometry controls carbon sink partitioning between above-ground tree biomass and soil organic matter in
 9 high fertility forests, *Iforest* 8, 195–206, doi:10.3832/ifor1196-008, 2014.
- 10 Aubinet M., Grelle G., Ibrom A., Rannik U., Moncrieff J., Foken T., Kowalski A. S., Martin P. H., Berbigier P.,
 11 Bernhofer C., Clement R., Elbers J., Granier A., Grunwald T., Morgenstern K., Pilegaard K., Rebmann C.,
 12 Snijders W., Valentini R. and Vesala T.: Estimates of the annual net carbon and water exchange of European
 13 forests: the EUROFLUX methodology, *Adv. Ecol. Res.*, 30, 113–175, doi:10.1016/S0065-2504(08)60018-5,
 14 2000.
- 15 Atkin, O. K., Atkinson, L. J., Fisher, R. A., Campbell, C. D., Zaragoza-Castells, J., Pitchford, J. W., Woodward,
 16 F. I. and Hurry, V.: Using temperature-dependent changes in leaf scaling relationships to quantitatively account
 17 for thermal acclimation of respiration in a coupled global climate-vegetation model, *Glob. Chang. Biol.*, 14, 1–
 18 18, doi:10.1111/j.1365-2486.2008.01664.x, 2008.
- 19 Baldocchi, D., Falge, E., Gu, L., Olson, R., Hollinger, D., Running, S., Anthoni, P., Bernhofer, C., Davis, K.,
 20 Evans, R., Fuentes, J., Goldstein, A., Katul, G., Law, B., Lee, X., Malhi, Y., Meyers, T., Munger, W., Oechel,
 21 W., Paw U, K. T., Pilegaard, K., Schmid, H. P., Valentini, R., Verma, S., Vesala, T., Wilson, K. and Wofsy, S.:
 22 FLUXNET: A new tool to study the temporal and spatial variability of ecosystem-scale carbon dioxide, water
 23 vapor, and energy flux densities, *Bull. Am. Meteorol. Soc.*, 82, 2415–2434, doi:10.1175/1520-
 24 0477(2001)082<2415:FANTTS>2.3.CO;2, 2001.
- 25 Ball, J. T., Woodrow, I. E. and Berry, J. A.: A model predicting stomatal conductance and its contribution to the
 26 control of photosynthesis under different environmental conditions, in *Progress in Photosynthesis Research*,
 27 edited by J. Biggins, pp. 221–224, Springer Netherlands., 1987.
- 28 Balogh, J., Pintér, K., Fóti, S., Cserhalmi, D., Papp, M. and Nagy, Z.: Dependence of soil respiration on soil
 29 moisture, clay content, soil organic matter, and CO₂ uptake in dry grasslands, *Soil Biol. Biochem.*, 43, 1006–
 30 1013, doi:10.1016/j.soilbio.2011.01.017, 2011.
- 31 Balsamo, G., Beljaars, A., Scipal, K., Viterbo, P., van den Hurk, B., Hirschi, M. and Betts, A. K.: A Revised
 32 Hydrology for the ECMWF Model: Verification from Field Site to Terrestrial Water Storage and Impact in the
 33 Integrated Forecast System, *J. Hydrometeorol.*, 10, 623–643, doi:10.1175/2008JHM1068.1, 2009.
- 34 Barcza, Z., Kern, A., Haszpra, L. and Kljun, N.: Spatial representativeness of tall tower eddy covariance
 35 measurements using remote sensing and footprint analysis, *Agric. For. Meteorol.*, 149, 795–807,
 36 doi:10.1016/j.agrformet.2008.10.021, 2009.



- 1 Barcza, Z., Bondeau, A., Churkina, G., Ciais, P., Czóbel, S., Gelybó, G., Grosz, B., Haszpra, L., Hidy, D.,
2 Horváth, L., Machon, A., Pásztor, L., Somogyi, Z. and Van Oost, K.: Model-based biospheric greenhouse gas
3 balance of Hungary, in *Atmospheric Greenhouse Gases: The Hungarian Perspective*, edited by L. Haszpra, pp.
4 295–330, Springer., 2011.
- 5 Beven, K. and Binley, A.: The future of distributed models: Model calibration and uncertainty prediction,
6 *Hydrol. Process.*, 6, 279–298, doi:10.1002/hyp.3360060305, 1992.
- 7 van Bodegom, P. M., Douma, J. C., Witte, J. P. M., Ordóñez, J. C., Bartholomeus, R. P., and Aerts, R.: Going
8 beyond limitations of plant functional types when predicting global ecosystem–atmosphere fluxes: exploring the
9 merits of traits-based approaches, *Global Ecol. Biogeogr.*, 21, 625–636, doi:10.1111/j.1466-8238.2011.00717.x,
10 2012.
- 11 Bond-Lamberty, B., Gower, S. T. and Ahl, D. E.: Improved simulation of poorly drained forests using Biome-
12 BGC, *Tree Physiol.*, 27, 703–715, doi:10.1093/treephys/27.5.703, 2007.
- 13 Campioli, M., Vicca, S., Luyssaert, S., Bilcke, J., Ceschia, E., Chapin III, F. S., Ciais, P., Fernández-Martínez,
14 M., Malhi, Y., Obersteiner, M., Olefeldt, D., Papale, D., Piao, S. L., Peñuelas, J., Sullivan, P. F., Wang, X.,
15 Zenone, T. and Janssens, I. A.: Biomass production efficiency controlled by management in temperate and
16 boreal ecosystems, *Nat. Geosci.*, 8, 843–846, doi:10.1038/ngeo2553, 2015.
- 17 Campbell, G. S. and Diaz, R.: Simplified soil water balance models to predict crop transpiration, in *Drought*
18 *Research Priorities for the Drylands*, pp. 15–26., 1988.
- 19 Cannell, M. G. R. and Thornley, J. H. M.: Modelling the components of plant respiration: Some guiding
20 principles, *Ann Bot-London*, 85, 45–54, doi:10.1006/anbo.1999.0996, 2000.
- 21 Chen, F. and Dudhia, J.: Coupling an Advanced Land Surface–Hydrology Model with the Penn State–NCAR
22 MM5 Modeling System. Part I: Model Implementation and Sensitivity, *Mon. Weather Rev.*, 129, 569–585,
23 doi:10.1175/1520-0493(2001)129<0569:CAALSH>2.0.CO;2, 2001.
- 24 Chiesi, M., Maselli, F., Moriondo, M., Fibbi, L., Bindi, M. and Running, S. W.: Application of BIOME-BGC to
25 simulate Mediterranean forest processes, *Ecol. Modell.*, 206, 179–190, doi:10.1016/j.ecolmodel.2007.03.032,
26 2007.
- 27 Churkina, G., Running, S. W., Running, S. W., Schloss, A. L. and the participants of the Potsdam NPP Model
28 Intercomparison: Comparing global models of terrestrial net primary productivity (NPP): the importance of
29 water availability, *Glob. Chang. Biol.*, 5, 46–55, doi:10.1046/j.1365-2486.1999.00006.x, 1999.
- 30 Churkina, G., Tenhunen, J., Thornton, P., Falge, E. M., Elbers, J. A., Erhard, M., Grünwald, T., Kowalski, A. S.,
31 Rannik, Ü. and Sprinz, D.: Analyzing the ecosystem carbon dynamics of four European coniferous forests using
32 a biogeochemistry model, *Ecosystems*, 6, 168–184, doi:10.1007/s10021-002-0197-2, 2003.
- 33 Churkina, G., Brovkin, V., von Bloh, W., Trusilova, K., Jung, M. and Dentener, F.: Synergy of rising nitrogen
34 depositions and atmospheric CO₂ on land carbon uptake moderately offsets global warming, *Global*
35 *Biogeochem. Cycles*, 23, GB4027, doi:10.1029/2008GB003291, 2009.
- 36 Churkina, G., Zaehle, S., Hughes, J., Viovy, N., Chen, Y., Jung, M., Heumann, B. W., Ramankutty, N.,
37 Heimann, M. and Jones, C.: Interactions between nitrogen deposition, land cover conversion, and climate change
38 determine the contemporary carbon balance of Europe, *Biogeosciences*, 7, 2749–2764, doi:10.5194/bg-7-2749-
39 2010, 2010.



- 1 Ciais, P., Sabine, C., Bala, G., Bopp, L., Brovkin, V., Canadell, J., Chhabra, A., DeFries, R., Galloway, J.,
 2 Heimann, M., Jones, C., Le Quéré, C., Myneni, R. B., Piao S., and Thornton, P.: Carbon and Other
 3 Biogeochemical Cycles, in *Climate Change 2013: The Physical Science Basis. Contribution of Working Group I*
 4 *to the Fifth Assessment Report of the Intergovernmental Panel on Climate Change* edited by T. F. Stocker, D.
 5 Qin, G. K. Plattner, M. Tignor, S. K. Allen, J. Boschung, A. Nauels, Y. Xia, V. Bex and P. M. Midgley,
 6 Cambridge University Press, Cambridge, United Kingdom and New York, NY, USA, 2013.
- 7 Chapin, F. S., Woodwell, G. M., Randerson, J. T., Rastetter, E. B., Lovett, G. M., Baldocchi, D. D., Clark, D. A.,
 8 Harmon, M. E., Schimel, D. S., Valentini, R., Wirth, C., Aber, J. D., Cole, J. J., Goulden, M. L., Harden, J. W.,
 9 Heimann, M. R., Howarth, W., Matson, P. A., McGuire, A. D., Melillo, J. M., Mooney, H. A., Neff, J. C.,
 10 Houghton, R. A., Pace, M. L., Ryan, M. G., Running, S. W., Sala, O. E., Schlesinger, W. H. and Schulze, E. D.:
 11 Reconciling carbon-cycle concepts, terminology, and methods, *Ecosystems* 9, 1041–1050, doi:10.1007/s10021-
 12 005-0105-7, 2006.
- 13 Clapp, R. B. and Hornberger, G. M.: Empirical equations for some soil hydraulic properties, *Water Resour. Res.*,
 14 14, 601–604, doi:10.1029/WR014i004p00601, 1978.
- 15 Collatz, G. J., Ball, J. T., Grivet, C. and Berry, J.: Physiological and environmental regulation of stomatal
 16 conductance, photosynthesis and transpiration: a model that includes a laminar boundary layer, *Agric. For.*
 17 *Meteorol.*, 54, 107–136, doi:10.1016/0168-1923(91)90002-8, 1991.
- 18 Damour, G., Simonneau, T., Cochard, H. and Urban, L.: An overview of models of stomatal conductance at the
 19 leaf level, *Plant. Cell Environ.*, 33, 1419–1438, doi:10.1111/j.1365-3040.2010.02181.x, 2010.
- 20 Driessen, P., Deckers, J., Spaargaren, O. and Nachtergaele, F.: Lecture notes on the major soils of the world,
 21 edited by P. Driessen, J. Deckers, O. Spaargaren, and F. Nachtergaele, Food and Agriculture Organization
 22 (FAO), 2001.
- 23 Eastaugh, C. S., Pötzelberger, E. and Hasenauer, H.: Assessing the impacts of climate change and nitrogen
 24 deposition on Norway spruce (*Picea abies* L. Karst) growth in Austria with BIOME-BGC, *Tree Physiol.*, 31,
 25 262–274, doi:10.1093/treephys/tpr033, 2011.
- 26 Farquhar, G. D., von Caemmerer, S. and Berry, J. A.: A bio-chemical model of photosynthetic CO₂ assimilation
 27 in leaves of C3 species, *Planta*, 149, 78–90, doi:10.1007/BF00386231, 1980.
- 28 Florides, G. and Kalogirou, S.: Annual ground temperature measurements at various depth, Available online:
 29 <https://www.researchgate.net/publication/30500353>, 2016.
- 30 Fodor, N. and Rajkai, K.: Computer program (SOILarium 1.0) for estimating the physical and hydrophysical
 31 properties of soils from other soil characteristics, *Agrokémia és Talajt.*, 60, 27–40, 2011.
- 32 Friedlingstein, P., Joel, G., Field, C. B. and Fung, I. Y.: Toward an allocation scheme for global terrestrial
 33 carbon models, *Glob. Chang. Biol.*, 5, 755–770, doi:10.1046/j.1365-2486.1999.00269.x, 1999.
- 34 Friedlingstein, P., Cox, P., Betts, R., Bopp, L., Von Bloh, W., Brovkin, V., Cadule, P., Doney, S., Eby, M.,
 35 Fung, I., Bala, G., John, J. J., Jones, C. J., Joos, F., Kato, T. K., Kawamiya, M., Knorr, W., Lindsay, K.,
 36 Matthews, H. D., Raddatz, T., Rayner, P., Reick, C., Roeckner, E., Schnitzler, K. G., Schnur, R., Strassmann, K.,
 37 Weaver, A.J., Yoshikawa, C. and Zeng, N.: Climate-carbon cycle feedback analysis: results from the C4MIP
 38 model intercomparison, *J. Clim.*, 19, 3338–3353, doi:10.1175/JCLI3800.1, 2006.



- 1 Friedlingstein, P. and Prentice, I. C.: Carbon-climate feedbacks: a review of model and observation based
2 estimates, *Curr. Opin. Environ. Sust.*, 2, 251–257, doi:10.1016/j.cosust.2010.06.002, 2010.
- 3 Friend, A. D., Arneeth, A., Kiang, N. Y., Lomas, M., Ogée, J., Rödenbeck, C., Running, S. W., Santaren, J. D.,
4 Sitch, S., Viovy, N., Woodward, F. I. and Zaehle, S.: FLUXNET and modelling the global carbon cycle, *Glob.*
5 *Chang. Biol.*, 1, 1–24, doi:10.1111/j.1365-2486.2006.01223.x, 2006.
- 6 Franks, P. J., Adams, M. A., Amthor, J. S., Barbour, M. M., Berry, J. A., Ellsworth, D. S., Farquhar, G. D.,
7 Ghannoum, O., Lloyd, J., McDowel, L., Norby, R. J., Tissue, D. T. and von Caemmerer, S.: Sensitivity of plants
8 to changing atmospheric CO₂ concentration: from the geological past to the next century, *New Phytol.*, 197,
9 1077–1094, doi:10.1111/nph.12104, 2013.
- 10 Foken, T. and Vichura, B.: Tools for quality assessment of surface-based flux measurements, *Agric. For.*
11 *Meteorol.*, 78, 83–105, doi:10.1016/0168-1923(95)02248-1, 1996.
- 12 Groffman, P. M. and Tiedje, J. M.: Denitrification in north temperate forest soils: Relationships between
13 denitrification and environmental factors at the landscape scale, *Soil Biol. Biochem.*, 21, 621–626,
14 doi:10.1016/0038-0717(89)90054-0, 1989
- 15 Hartig, F., Dyke, J., Hickler, T., Higgins, S. I., O’Hara, R. B., Scheiter, S. and Huth, A.: Connecting dynamic
16 vegetation models to data - an inverse perspective, *J. Biogeogr.*, 39, 2240–2252, doi:10.1111/j.1365-
17 2699.2012.02745.x, 2012.
- 18 Hashimoto, S., Morishita, T., Sakata, T., Ishizuka, S., Kaneko, S. and Takahashi, M.: Simple models for soil
19 CO₂, CH₄, and N₂O fluxes calibrated using a Bayesian approach and multi-site data, *Ecol. Modell.*, 222, 1283–
20 1292, doi:10.1016/j.ecolmodel.2011.01.013, 2011.
- 21 Hidy, D., Barcza, Z., Haszpra, L., Churkina, G., Pintér, K. and Nagy, Z.: Development of the Biome-BGC model
22 for simulation of managed herbaceous ecosystems, *Ecol. Modell.*, 226, 99–119,
23 doi:10.1016/j.ecolmodel.2011.11.008, 2012.
- 24 Hidy, D., Barcza, Z., Thornton, P. and Running, S. W.: User’s Guide for Biome-BGC MuSo 4.0. Available
25 online: http://nimbus.elte.hu/bbgc/files/Manual_BBGC_MuSo_v4.0.pdf, 2015
- 26 Hlásny, T., Barcza, Z., Barka, I., Merganicova, K., Sedmak, R., Kern, A., Pajtik, J., Balazs, B., Fabrika, M. and
27 Churkina, G.: Future carbon cycle in mountain spruce forests of Central Europe: Modelling framework and
28 ecological inferences, *For. Ecol. Manage.*, 328, 55–68, doi:10.1016/j.foreco.2014.04.038, 2014.
- 29 Hunt, E. R., Piper, S. C., Nemani, R., Keeling, C. D., Otto, R. D. and Running, S. W.: Global net carbon
30 exchange and intra-annual atmospheric CO₂ concentrations predicted by an ecosystem process model and three-
31 dimensional atmospheric transport model, *Global Biogeochem. Cycles*, 10, 431–456, doi:10.1029/96GB01691,
32 1996.
- 33 Huntzinger, D. N., Schwalm, C., Michalak, A. M., Schaefer, K., King, A. W., Wei, Y., Jacobson, A., Liu, S.,
34 Cook, R. B., Post, W. M., Berthier, G., Hayes, D., Huang, M., Ito, A., Lei, H., Lu, C., Mao, J., Peng, C. H.,
35 Peng, S., Poulter, B., Ricciuto, D., Shi, X., Tian, H., Wang, W., Zenh, N., Zhao, F. and Zhu, Q.: The North
36 American Carbon Program Multi-Scale Synthesis and Terrestrial Model Intercomparison Project - Part 1:
37 Overview and experimental design, *Geosci. Model Dev.*, 6, 2121–2133, doi:10.5194/gmd-6-2121-2013, 2013.
- 38



- 1 IPCC Guidelines for National Greenhouse Gas Inventories, edited by H. S. Eggleston, L. Buendia, K. Miwa, T.
 2 Ngara and K. Tanabe, National Greenhouse Gas Inventories Programme, IGES, Japan, 2006.
- 3 Jarvis, P. G.: The interpretation of the variations in leaf water potential and stomatal conductance found in
 4 canopies in the field, *Philos. Trans. R. Soc. B*, 273, 593–610, doi:10.1098/rstb.1976.0035, 1976.
- 5 Jarvis, N. J.: A simple empirical model of root water uptake, *J. Hydrol.*, 107, 57–72, doi:10.1016/0022-
 6 1694(89)90050-4, 1989.
- 7 Jochheim, H., Puhlmann, M., Beese, F., Berthold, D., Einert, P., Kallweit, R., Konopatzky, A., Meesenburg, H.,
 8 Meiwes, K. J., Raspe, S., Schulte-Bisping, H. and Schulz, C.: Modelling the carbon budget of intensive forest
 9 monitoring sites in Germany using the simulation model BIOME-BGC, *Biogeosciences For.*, 2, 7–10,
 10 doi:10.3832/ifer0475-002, 2009.
- 11 Jolly, W., Nemani, R. R. and Running, S. W.: A generalized, bioclimatic index to predict foliar phenology in
 12 response to climate, *Glob. Chang. Biol.*, 11, 619–632, doi:0.1111/j.1365-2486.2005.00930.x, 2005.
- 13 Jung, M., Le Maire, G., Zaehle, S., Luyssaert, S., Vetter, M., Churkina, G., Ciais, P., Viovy, N. and Reichstein,
 14 M.: Assessing the ability of three land ecosystem models to simulate gross carbon uptake of forests from boreal
 15 to Mediterranean climate in Europe, *Biogeosciences*, 4, 647–656, doi:10.5194/bgd-4-1353-2007, 2007a.
- 16 Jung, M., Vetter, M., Herold, M., Churkina, G., Reichstein, M., Zaehle, S., Ciais, P., Viovy, N., Bondeau, A.,
 17 Chen, Y., Trusilova, K., Feser, F. and Heimann, M.: Uncertainties of modeling gross primary productivity over
 18 Europe: A systematic study on the effects of using different drivers and terrestrial biosphere models, *Global*
 19 *Biogeochem. Cycles*, 21, GB4021, doi:10.1029/2006GB002915, 2007b.
- 20 Kattge, J., Díaz, S., Lavorel, S., Prentice, I. C., Leadley, P., Bönisch, G., Garnier, E., Westoby, M., Reich, P. B.,
 21 Wright, I. J., Cornelissen, J. H. C., Violle, C., Harrison, S. P., Van Bodegom, P. M., Reichstein, M., Enquist, B.
 22 J., Soudzilovskaia, N. A., Ackerly, D. D., Anand, M., Atkin, O., Bahn, M., Baker, T. R., Baldocchi, D., Bekker,
 23 R., Blanco, C. C., Blonder, B., Bond, W. J., Bradstock, R., Bunker, D. E., Casanoves, F., Cavender-Bares, J.,
 24 Chambers, J. Q., Chapin, F. S., Chave, J., Coomes, D., Cornwell, W. K., Craine, J. M., Dobrin, B. H., Duarte, L.,
 25 Durka, W., Elser, J., Esser, G., Estiarte, M., Fagan, W. F., Fang, J., Fernández-Méndez, F., Fidelis, A., Finegan,
 26 B., Flores, O., Ford, H., Frank, D., Freschet, G. T., Fyllas, N. M., Gallagher, R. V., Green, W. A., Gutierrez, A.
 27 G., Hickler, T., Higgins, S. I., Hodgson, J. G., Jalili, A., Jansen, S., Joly, C. A., Kerkhoff, A. J., Kirkup, D.,
 28 Kitajima, K., Kleyer, M., Klotz, S., Knops, J. M. H., Kramer, K., Kühn, I., Kurokawa, H., Laughlin, D., Lee, T.
 29 D., Leishman, M., Lens, F., Lenz, T., Lewis, S. L., Lloyd, J., Llusià, J., Louault, F., Ma, S., Mahecha, M. D.,
 30 Manning, P., Massad, T., Medlyn, B. E., Messier, J., Moles, A. T., Müller, S. C., Nadrowski, K., Naeem, S.,
 31 Niinemets, Ü., Nöllert, S., Nüske, A., Ogaya, R., Oleksyn, J., Onipchenko, V. G., Onoda, Y., Ordoñez, J.,
 32 Overbeck, G., Ozinga, W. A., Patiño, S., Paula, S., Pausas, J. G., Peñuelas, J., Phillips, O. L., Pillar, V., Poorter,
 33 H., Poorter, L., Poschlod, P., Prinzing, A., Proulx, R., Rammig, A., Reinsch, S., Reu, B., Sack, L., Salgado-
 34 Negret, B., Sardans, J., Shiodera, S., Shipley, B., Siefert, A., Sosinski, E., Soussana, J. F., Swaine, E., Swenson,
 35 N., Thompson, K., Thornton, P., Waldram, M., Weiher, E., White, M., White, S., Wright, S. J., Yguel, B.,
 36 Zaehle, S., Zanne, A. E. and Wirth, C.: TRY - a global database of plant traits, *Glob. Chang. Biol.*, 17, 2905–
 37 2935, doi:10.1111/j.1365-2486.2011.02451.x, 2011.
- 38 Kimball, J. S., White, M. A. and Running, S. W.: BIOME-BGC simulations of stand hydrologic processes for
 39 BOREAS, *J. Geophys. Res.*, 102(D24), 29043–29051, doi:10.1029/97JD02235, 1997.



- 1 Knorr, W. and Kattge, J.: Inversion of terrestrial ecosystem model parameter values against eddy covariance
 2 measurements by Monte Carlo sampling, *Glob. Chang. Biol.*, 11, 1333–1351, doi:10.1111/j.1365-
 3 2486.2005.00977.x, 2005.
- 4 Korol, R. L., Milner, K. S. and Running, S. W.: Testing a mechanistic model for predicting stand and tree
 5 growth, *For. Sci.*, 42, 139–153, 1996.
- 6 Kulkarni, M. V., Burgin, A. J., Groffman, P. M. and Yavitt, J. B.: Direct flux and N-15 tracer methods for
 7 measuring denitrification in forest soils, *Biogeochemistry*, 117, 359–373, doi:10.1007/s10533-013-9876-7, 2014.
- 8 Lagergren, F., Grelle, A., Lankreijer, H., Mölder, M. and Lindroth, A.: Current carbon balance of the forested
 9 area in Sweden and its sensitivity to global change as simulated by Biome-BGC, *Ecosystems*, 9, 894–908,
 10 doi:10.1007/s10021-005-0046-1, 2006.
- 11 Leuning, R.: A critical appraisal of a combined stomatal-photosynthesis model for C3 plants, *Plant. Cell*
 12 *Environ.*, 18, 339–355, doi:10.1111/j.1365-3040.1995.tb00370.x, 1995.
- 13 Liu, H. P., Peters G. and Foken, T.: New equations for sonic temperature variance and buoyancy heat flux with
 14 an omnidirectional sonic anemometer, *Bound.-Layer Meteor.*, 100, 459–468, doi:10.1023/A:1019207031397,
 15 2001.
- 16 Lombardozi, D. L., Bonan, G. B., Smith, N. G., Dukes, J. S. and Fisher, R. A.: Temperature acclimation of
 17 photosynthesis and respiration: a key uncertainty in the carbon cycle-climate feedback, *Geophys. Res. Lett.*, 42,
 18 8624–8631, doi:10.1002/2015GL065934, 2015.
- 19 Ma, S., Churkina, G., Wieland, R. and Gessler, A.: Optimization and evaluation of the ANTHRO-BGC model
 20 for winter crops in Europe, *Ecol. Modell.*, 222, 3662–3679, doi:10.1016/j.ecolmodel.2011.08.025, 2011.
- 21 Ma, S., Acutis, A., Barcza, Z., Touhami, H. B., Doro, L., Hidy, D., Köchy, M., Minet, J., Lellei-Kovács, E.,
 22 Perego, A., Rolinski, A., Ruget, F., Seddaiu, G., Wu, L. and Bellocchi, G.: The grassland model intercomparison
 23 of the MACSUR (Modelling European Agriculture with Climate Change for Food Security) European
 24 knowledge hub, in *Proceedings of the 7th International Congress on Environmental Modelling and Software*,
 25 edited by D. P. Ames, N. W. T. Quinn, A. E. Rizzoli, San Diego, California, USA, 2014.
- 26 Marjanović, H., Alberti, G., Balogh, J., Czóbel, S., Horváth, L., Jagodics, A., Nagy, Z., Ostrogović, M. Z.,
 27 Peressotti, A. and Führer, E.: Measurements and estimations of biosphere-atmosphere exchange of greenhouse
 28 gases – Grasslands, in *Atmospheric Greenhouse Gases: The Hungarian Perspective*, edited by L. Haszpra, pp.
 29 121–156, Springer, Dordrecht - Heidelberg - London - New York, doi:10.1007/978-90-481-9950-1_7, 2011a.
- 30 Marjanović, H., Ostrogović, M. Z., Alberti, G., Balenović, I., Paladinić, E., Indir, K., Peressotti, A. and Vuletić,
 31 D.: Carbon dynamics in younger stands of pedunculate oak during two vegetation periods, *Šum. list special*
 32 *issue*, 135, 59–73, 2011b. (in Croatian with English summary)
- 33 Martre, P., Wallach, D., Asseng, S., Ewert, F., Jones, J. W., Rotter, R. P., Boote, K. J., Ruane, A. C., Thorburn,
 34 P. J., Cammarano, D., Hatfield, J. L., Rosenzweig, C., Aggarwal, P. K., Angulo, C., Basso, B., Bertuzzi, P.,
 35 Biernath, C., Brisson, N., Challinor, A. J., Doltra, J., Gayler, S., Goldberg, R., Grant, R. F., Heng, L., Hooker, J.,
 36 Hunt, L. A., Ingwersen, J., Izaurralde, R. C., Kersebaum, K. C., Müller, C., Kumar, S. N., Nendel, C., O’leary,
 37 G., Olesen, J. E., Osborne, T. M., Palosuo, T., Priesack, E., Ripoche, D., Semenov, M. A., Shcherback, I.,
 38 Steduto, P., Stöckle, C. O., Stratonovitch, P., Streck, T., Supit, I., Tao, F., Travasso, M., Waha, K., White, J.W.



- 1 and Wolf, J.: Multimodel ensembles of wheat growth: many models are better than one, *Glob. Chang. Biol.*, 21,
2 911-925, doi:10.1111/gcb.12768, 2015.
- 3 Maselli, F., Chiesi, M., Brilli, L. and Moriondo, M.: Simulation of olive fruit yield in Tuscany through the
4 integration of remote sensing and ground data, *Ecol. Modell.*, 244, 1–12, doi:10.1016/j.ecolmodel.2012.06.028,
5 2012.
- 6 Massman W.J.: The attenuation of concentration fluctuations in turbulent flow through a tube, *J. Geophys. Res.*,
7 96(D8), 15269-15273, doi:10.1029/91JD01514, 1991.
- 8 Mayer, B.: Hydropedological relations in the region of lowland forests of Pokupsko basin, Radovi Šumarskog
9 instituta Jastrebarsko, 31, 37–89, 1996. (in Croatian with English summary)
- 10 Medlyn, B. E., Dreyer, E., Ellsworth, D., Forstreuter, M., Harley, P. C., Kirschbaum, M. U. F., Le Roux, X.,
11 Montpied, P., Strassmeyer, J., Walcroft, A., Wang, K., Loustau, D.: Temperature response of parameters of a
12 biochemically based model of photosynthesis. II. A review of experimental data, *Plant, Cell Environ.*, 25, 1167–
13 1179, doi:10.1046/j.1365-3040.2002.00891.x, 2002.
- 14 Merganičová, K., Pietsch, S. A. and Hasenauer, H.: Testing mechanistic modeling to assess impacts of biomass
15 removal, *For. Ecol. Manage.*, 207, 37–57, doi:10.1016/j.foreco.2004.10.017, 2005.
- 16 van der Molen, M. K., Gash, J. H. C. and Elbers, J. A.: Sonic anemometer (co)sine response and flux
17 measurement - II. The effect of introducing an angle of attack dependent calibration, *Agric. For. Meteorol.*, 122,
18 95-109, 2004.
- 19 van der Molen, M. K., Dolman, A. J., Ciais, P., Eglin, T., Gobron, N., Law, B. E., Meir, P., Peters, W., Phillips,
20 O. L., Reichstein, M., Chen, T., Dekker, S. C., Doubková, M., Friedl, M. A., Jung, M., van den Hurk, B. J. J.
21 M., de Jeu, R. A. M., Kruijt, B., Ohta, T., Rebel, K. T., Plummer, S., Seneviratne, S. I., Sitch, S., Teuling, A. J.,
22 van der Werf, G. R. and Wang, G.: Drought and ecosystem carbon cycling, *Agric. For. Meteorol.*, 151, 765–773,
23 doi:10.1016/j.agrformet.2011.01.018, 2011.
- 24 Morecroft, M. D.; Roberts, J. M.: Photosynthesis and stomatal conductance of mature canopy Oak and Sycamore
25 trees throughout the growing season. *Functional Ecology*, 13(3), 332-342, 1999.
- 26 Moore, C. J.: Frequency-response corrections for eddy-correlation systems, *Bound.-Layer Meteorol.*, 37, 17–35,
27 doi:10.1007/BF00122754, 1986.
- 28 Mu, Q., Zhao, M., Running, S. W., Liu, M. and Tian, H.: Contribution of increasing CO₂ and climate change to
29 the carbon cycle in China's ecosystems, *J. Geophys. Res. Biogeosciences*, 113, G01018,
30 doi:10.1029/2006JG00316, 2008.
- 31 Nakai, T., van der Molen, M. K., Gash, J. H. C., & Kodama, Y: Correction of sonic anemometer angle of attack
32 errors, *Agricultural and Forest Meteorology*, 136(1–2), 19–30. doi: 10.1016/j.agrformet.2006.01.006, 2006.
- 33 Ritchie, J. T.: Soil water balance and plant water stress. In *Understanding Options for Agricultural Production*,
34 edited by Tsuji, G. Y., Hoogenboom, G., Thornton, P.E., pp. 41–54, Kluwer Academic Publishers, The
35 Netherlands, 1998.
- 36 Nagy, Z., Pintér, K., Czóbel, S., Balogh, J., Horváth, L., Fóti, S., Barcza, Z., Weidinger, T., Csintalan, Z., Dinh,
37 N. Q., Grosz, B. and Tuba, Z.: The carbon budget of semi-arid grassland in a wet and a dry year in Hungary,
38 *Agric. Ecosyst. Environ.*, 121, 21–29, doi:10.1016/j.agee.2006.12.003, 2007.



- 1 Nagy, Z., Barcza, Z., Horváth, L., Balogh, J., Hagyó, A., Káposztás, N., Grosz, B., Machon, A. and Pintér, K.:
- 2 Measurements and estimations of biosphere-atmosphere exchange of greenhouse gases – Grasslands, in
- 3 Atmospheric Greenhouse Gases: The Hungarian Perspective, edited by L. Haszpra, pp. 91–120, Springer,
- 4 Dordrecht - Heidelberg - London - New York., 2011.
- 5 Nemani, R. R. and Running, S. W.: Testing a theoretical climate-soil-leaf area hydrologic equilibrium of forests
- 6 using satellite data and ecosystem simulation, *Agric. For. Meteorol.*, 44, 245–260, doi:10.1016/0168-
- 7 1923(89)90020-8, 1989.
- 8 Olin, S., Schurgers, G., Lindeskog, M., Wårlind, D., Smith, B., Bodin, P., Holmér J. and Arneft, A.: Modelling
- 9 the response of yields and tissue C:N to changes in atmospheric CO₂ and N management in the main wheat
- 10 regions of western Europe, *Biogeosciences*, 12, 2489–2515, doi:10.5194/bg-12-2489-2015, 2015.
- 11 Ostrogović, M. Z.: Carbon stocks and carbon balance of an even-aged pedunculate oak (*Quercus robur* L.) forest
- 12 in Kupa river basin, doctoral thesis, Faculty of forestry, University of Zagreb, 2013. (in Croatian with English
- 13 summary)
- 14 Petritsch, R., Hasenauer, H. and Pietsch, S. A.: Incorporating forest growth response to thinning within biome-
- 15 BGC, *For. Ecol. Manage.*, 242, 324–336, doi:10.1016/j.foreco.2007.01.050, 2007.
- 16 Pietsch, S. A., Hasenauer, H., Kucera, J. and Cermák, J.: Modeling effects of hydrological changes on the carbon
- 17 and nitrogen balance of oak in floodplains, *Tree Physiol.*, 23, 735–746, 2003.
- 18 Reichstein, M., Falge, E., Baldocchi, D., Papale, D., Aubinet, M., Berbigier, P., Bernhofer, C., Buchmann, N.,
- 19 Gilmanov, T., Granier, A., Grunwald, T., Havrankova, K., Ilvesniemi, H., Janous, D., Knohl, A., Laurila, T.,
- 20 Lohila, A., Loustau, D., Matteucci, G., Meyers, T., Miglietta, F., Ourcival, J.M., Pumpanen, J., Rambal, S.,
- 21 Rotenberg, E., Sanz, M., Tenhunen, J., Seufert, G., Vaccari, F., Vesala, T., Yakir, D. and Valentini, R.: On the
- 22 separation of net ecosystem exchange into assimilation and ecosystem respiration: review and improved
- 23 algorithm, *Glob. Chang. Biol.*, 11, 1424–1439, doi:10.1111/j.1365-2486.2005.001002, 2005.
- 24 Running, S. W. and Coughlan, J. C.: A general model of forest ecosystem processes for regional applications I.
- 25 Hydrologic balance, canopy gas exchange and primary production processes, *Ecol. Modell.*, 42, 125– 154,
- 26 doi:10.1016/0304-3800(88)90112-3, 1988.
- 27 Running, S. W. and Gower, S. T.: FOREST-BGC, A general model of forest ecosystem processes for regional
- 28 applications. II. Dynamic carbon allocation and nitrogen budgets, *Tree Physiol.*, 9, 147–160,
- 29 doi:10.1093/treephys/9.1-2.147, 1991.
- 30 Running, S. W. and Hunt, E. R. J.: Generalization of a forest ecosystem process model for other biomes,
- 31 BIOME-BGC, and an application for global-scale models, in *Scaling Physiological Processes: Leaf to Globe*,
- 32 edited by J. R. Ehleringer and C. Field, pp. 141–158, Academic Press, San Diego, 1993.
- 33 Sándor, R. and Fodor, N.: Simulation of soil temperature dynamics with models using different concepts, *Sci.*
- 34 *World J.*, 2012, 1–8, doi:10.1100/2012/590287, 2012.
- 35 Sándor, R., Ma, S., Acutis, M., Barcza, Z., Ben Touhami, H., Doro, L., Hidy, D., Köchy, M., Lellei-Kovács, E.,
- 36 Minet, J., Perego, A., Rolinski, S., Ruget, F., Seddaiu, G., Wu, L. and Bellocchi, G.: Uncertainty in simulating
- 37 biomass yield and carbon-water fluxes from grasslands under climate change, *Adv. Anim. Biosci.*, 6, 49–51,
- 38 doi:10.1017/S2040470014000545, 2015.



- 1 Sándor, R., Barcza, Z., Hidy, D., Lellei-Kovács, E., Ma, S. and Bellocchi, G.: Modelling of grassland fluxes in
2 Europe: evaluation of two biogeochemical models, *Agric. Ecosyst. Environ.*, 215, 1–19,
3 doi:10.1016/j.agee.2015.09.001, 2016.
- 4 Schmid, S., Zierl, B. and Bugmann, H.: Analyzing the carbon dynamics of central European forests: comparison
5 of Biome-BGC simulations with measurements, *Reg. Environ. Chang.*, 6, 167–180, doi:10.1007/s10113-006-
6 0017-x, 2006.
- 7 Schulze, E. D., Luyssaert, S., Ciais, P., Freibauer, A., Janssens, I. A., Soussana, J. F., Smith, P., Grace, J., Levin,
8 I., Thiruchittampalam, B., Heimann, M., Dolman, A. J., Valentini, R., Bousquet, P., Peylin, P., Peters, W.,
9 Rödenbeck, C., Etiope, G., Vuichard, N., Wattenbach, M., Nabuurs, G. J., Poussi, Z., Nieschulze, J., Gash, J. H.,
10 and CarboEurope Team: Importance of methane and nitrous oxide for Europe’s terrestrial greenhouse-gas
11 balance, *Nature Geosci.*, 2, 842–850, doi:10.1038/ngeo686, 2009.
- 12 Schwalm, C. R., Williams, C. A., Schaefer, K., Anderson, R., Arain, M. A., Baker, I., Barr, A., Black, T. A.,
13 Chen, G., Chen, J. M., Ciais, P., Davis, K. J., Desai, A., Dietze, M., Dragoni, D., Fischer, M. L., Flanagan, L. B.,
14 Grant, R., Gu, L., Hollinger, D., Izaurralde, R. C., Kucharik, C., Lafleur, P., Law, B. E., Li, L., Li, Z., Liu, S.,
15 Lokupitiya, E., Luo, Y., Ma, S., Margolis, H., Matamala, R., McCaughey, H., Monson, R. K., Oechel, W. C.,
16 Peng, C., Poulter, B., Price, D. T., Riciutto, D. M., Riley, W., Sahoo, A. K., Sprintsin, M., Sun, J., Tian, H.,
17 Tonitto, C., Verbeeck, H. and Verma, S. B.: A model-data intercomparison of CO₂ exchange across North
18 America: Results from the North American Carbon Program site synthesis, *J. Geophys. Res.*, 115, G00H05,
19 doi:10.1029/2009JG001229, 2010.
- 20 Schwalm, C. R., Huntinzger, D. N., Fisher, J. B., Michalak, A. M., Bowman, K., Cias, P., Cook, R., El-Masri,
21 B., Hayes, D., Huang, M., Ito, A., Jain, A., King, A.W., Lei, H., Liu, J., Lu, C., Mao, J., Peng, S., Poulter, B.,
22 Ricciuto, D., Schaefer, K., Shi, X., Tao, B., Tian, H., Wang, W., Wei, Y., Yang, J. and Zeng, N.: Toward
23 “optimal” integration of terrestrial biosphere models, *Geophys. Res. Lett.*, 42, 4418–4428,
24 doi:10.1002/2015GL064002, 2015.
- 25 Smith, N. G. and Dukes, J. S.: Plant respiration and photosynthesis in global-scale models: Incorporating
26 acclimation to temperature and CO₂, *Glob. Chang. Biol.*, 19, 45–63, doi:10.1111/j.1365-2486.2012.02797.x,
27 2012.
- 28 Suyker A. E., Verma S. B. and Burba G. G.: Interannual variability in net CO₂ exchange of a native tallgrass
29 prairie, *Global Change Biol.*, 9, 255–265, doi:10.1046/j.1365-2486.2003.00567.x, 2003.
- 30 Suyker, A. E., Verma, S. B., Burba, G. G., Arkebauer, T. J., Walters, D. T. and Hubbard, K. G.: Growing season
31 carbon dioxide exchange in irrigated and rainfed maize, *Agric. For. Meteorol.*, 124, 1–13,
32 doi:10.1016/j.agrformet.2004.01.011, 2004.
- 33 Tatarinov, F. A. and Cienciala, E.: Application of BIOME-BGC model to managed forests, *For. Ecol. Manage.*,
34 237, 267–279, doi:10.1016/j.foreco.2006.09.085, 2006.
- 35 Thomas, R. Q., Bonan, G. B. and Goodale, C. L.: Insights into mechanisms governing forest carbon response to
36 nitrogen deposition: a model-data comparison using observed responses to nitrogen addition, *Biogeosciences*,
37 10, 3869–3887, doi:10.5194/bg-10-3869-2013, 2013.
- 38 Thornton, P. E.: Regional ecosystem simulation: Combining surface- and satellite-based observations to study
39 linkages between terrestrial energy and mass budgets, The University of Montana., 1998.



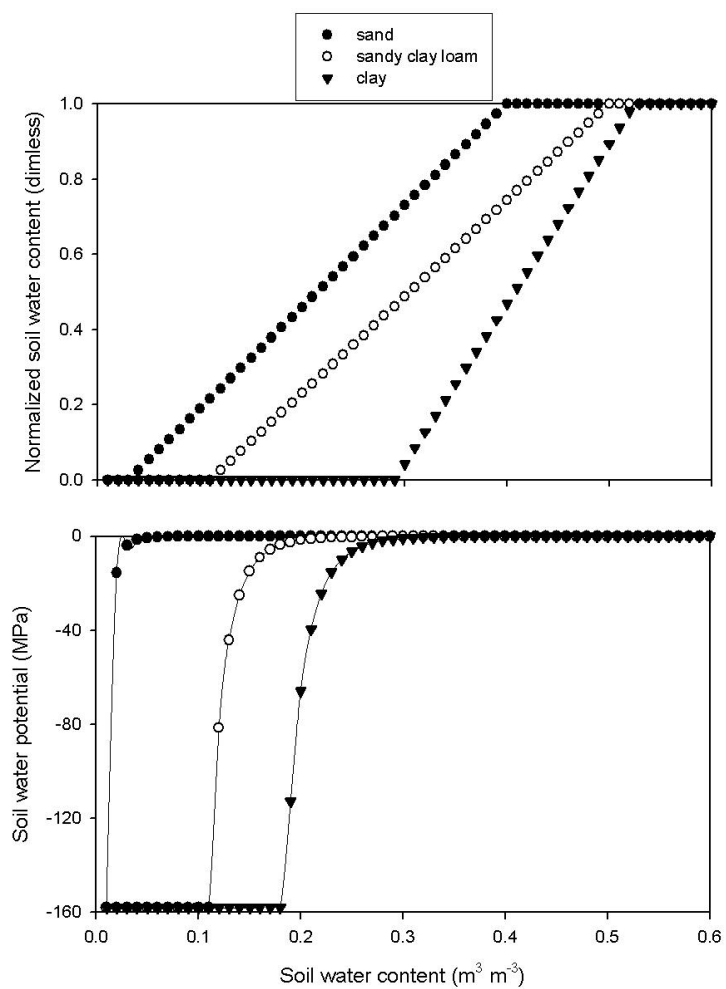
- 1 Thornton, P., Law, B., Gholz, H. L., Clark, K. L., Falge, E., Ellsworth, D., Goldstein, A., Monson, R., Hollinger,
2 D., Falk, M., Chen, J. and Sparks, J.: Modeling and measuring the effects of disturbance history and climate on
3 carbon and water budgets in evergreen needleleaf forests, *Agric. For. Meteorol.*, 113, 185–222,
4 doi:10.1016/S0168-1923(02)00108-9, 2002.
- 5 Thornton, P. E.: User's Guide for Biome-BGC, Version 4.1.1. [online] Available from:
6 ftp://daac.ornl.gov/data/model_archive/BIOME_BGC/biome_bgc_4.1.1/comp/bgc_users_guide_411.pdf, 2000.
- 7 Thornton, P. E. and Rosenbloom, N. A.: Ecosystem model spin-up: Estimating steady state conditions in a
8 coupled terrestrial carbon and nitrogen cycle model, *Ecol. Modell.*, 189, 25–48,
9 doi:10.1016/j.ecolmodel.2005.04.008, 2005.
- 10 Tjoelker, M. G., Oleksyn, J. and Reich, P. B.: Modelling respiration of vegetation: evi- dence for a general
11 temperature-dependent Q10, *Global Change Biol.*, 7, 223–230, doi:10.1046/j.1365-2486.2001.00397.x, 2001.
- 12 Trusilova, K. and Churkina, G.: The response of the terrestrial biosphere to urbanization: land cover conversion,
13 climate, and urban pollution, *Biogeosciences Discuss.*, 5, 2445–2470, doi:10.5194/bgd-5-2445-2008, 2008.
- 14 Trusilova, K., Trembath, J. and Churkina, G.: Parameter estimation and validation of the terrestrial ecosystem
15 model Biome-BGC using eddy-covariance flux measurements, Technical Report 16, MPI for Biogeochemistry,
16 Jena, 2009.
- 17 Ťupek, B., Zanchi, G., Verkerk, P. J., Churkina, G., Viovy, N., Hughes, J. K. and Lindner, M.: A comparison of
18 alternative modelling approaches to evaluate the European forest carbon fluxes, *For. Ecol. Manage.*, 260, 241–
19 251, doi:10.1016/j.foreco.2010.01.045, 2010.
- 20 Turner, D. P., Ritts, W. D., Law, B. E., Cohen, W. B., Yang, Z., Hudiburg, T., Campbell, J. L. and Duane, M.:
21 Scaling net ecosystem production and net biome production over a heterogeneous region in the western United
22 States, *Biogeosciences Discuss.*, 4, 1093–1135, doi:10.5194/bgd-4-1093-2007, 2007.
- 23 Ueyama, M., Ichii, K., Hirata, R., Takagi, K., Asanuma, J., Machimura, T., Nakai, Y., Ohta, T., Saigusa, N.,
24 Takahashi, T. and Hirano, T.: Simulating carbon and water cycles of larch forests in East Asia by the BIOME-
25 BGC model with AsiaFlux data, *Biogeosciences*, 7, 959–977, doi:10.5194/bg-7-959-2010, 2010.
- 26 Verma, S. B., Dobermann, A., Cassman, K. G., Walters, D. T., Knops, J. M. N., Arkebauer, T. J., Suyker, A. E.,
27 Burba, G., Amos, B., Yang, H., Ginting, D., Hubbard, K., Gitleson, A. A. and Walter-Shea E.A.: Annual carbon
28 dioxide exchange in irrigatedrainfed maize based agroecosystems, *Agr. Forest Meteorol.*, 131, 77–96,
29 doi:10.1016/j.agrformet.2005.05.003, 2005.
- 30 Vetter, M., Wirth, C., Böttcher, H., Churkina, G., Schulze, E.-D., Wutzler, T. and Weber, G.: Partitioning direct
31 and indirect human-induced effects on carbon sequestration of managed coniferous forests using model
32 simulations and forest inventories, *Global Change Biol.*, 11, 810–827, doi:10.1111/j.1365-2486.2005.00932.x,
33 2005.
- 34 Vetter, M., Churkina, G., Jung, M., Reichstein, M., Zaehle, S., Bondeau, A., Chen, Y., Ciais, P., Feser, F.,
35 Freibauer, A., Geyer, R., Jones, C., Papale, D., Tenhunen, J., Tomelleri, E., Trusilova, K., Viovy, N. and
36 Heimann, M.: Analyzing the causes and spatial pattern of the European 2003 carbon flux anomaly using seven
37 models, *Biogeosciences*, 5, 561–583, doi:10.5194/bg-5-561-2008, 2008.
- 38 Vickers, D. and Mahrt, L.: Quality control and flux sampling problems for tower and aircraft data, *J. Atmos.*
39 *Oceanic Technol.*, 14, 512–526, doi:10.1175/1520-0426(1997)014<0512:QCAFSP>2.0.CO;2, 1997.



- 1 Di Vittorio, A. V., Anderson, R. S., White, J. D., Miller, N. L. and Running, S. W.: Development and
2 optimization of an Agro-BGC ecosystem model for C4 perennial grasses, *Ecol. Modell.*, 221, 2038–2053,
3 doi:10.1016/j.ecolmodel.2010.05.013, 2010.
- 4 Vitousek, P. M., Fahey, T., Johnson, D. W. and Swift, M. J.: Element interactions in forest ecosystems:
5 succession, allometry and input-output budgets, *Biogeochemistry*, 5, 7–34, doi:10.1007/BF02180316, 1988.
- 6 Vitousek, P., Edin, L. O., Matson, P. A., Fownes, J. H. and Neff, J.: Within-system element cycles, input-output
7 budgets, and nutrient limitations, in *Success, Limitations, and Frontiers in Ecosystem Science*, edited by M. Pace
8 and P. Groffman, pp. 432–451, Springer, New York., 1998.
- 9 Wang, Q., Watanabe, M. and Ouyang, Z.: Simulation of water and carbon fluxes using BIOME-BGC model
10 over crops in China, *Agric. For. Meteorol.*, 131, 209–224, doi:10.1016/j.agrformet.2005.06.002, 2005.
- 11 Webb, E. K., Pearman, G. I. and Leuning, R.: Correction of flux measurements for density effects due to heat
12 and water-vapor transfer, *Q. J. R. Meteorolog. Soc.*, 106, 85–100, doi:10.1002/qj.49710644707, 1980.
- 13 White, A., Melvin, G. R., Cannell, A. and Friend, D.: Climate change impacts on ecosystems and the terrestrial
14 carbon sink: a new assessment, *Global Environ. Change*, 9, 21–30, doi:10.1016/S0959-3780(99)00016-3, 1999.
- 15 White, M., Thornton, P. E., Running, S. W. and Nemani, R. R.: Parameterization and sensitivity analysis of the
16 BIOME-BGC terrestrial ecosystem model: Net primary production controls, *Earth Interact.*, 4, 1–85,
17 doi:10.1175/1087-3562(2000)004<0003:PASAOT>2.0.CO;2, 2000.
- 18 Wilczak, J. M., Oncley, S. P. and Stage, S. A.: Sonic anemometer tilt correction algorithms, *Bound.-Layer
19 Meteorol.*, 99, 127–150, doi:10.1023/A:1018966204465, 2001.
- 20 Williams, J. R.: Runoff and water erosion, in *Modeling plant and soil systems. Agronomy Monograph nr. 31,*
21 edited by R. J. Hanks and J. T. Ritchie, pp. 439–455, American Society of Agronomy, Madison, Wisconsin,
22 USA., 1991.
- 23 Williams, M., Richardson, A. D., Reichstein, M., Stoy, P. C., Peylin, P., Verbeeck, H., Carvalhais, N., Jung, M.,
24 Hollinger, D. Y., Kattge, J., Leuning, R., Luo, Y., Tomelleri, E., Trudinger, C. and Wang, Y.-P.: Improving land
25 surface models with FLUXNET data, *Biogeosciences Discuss.*, 6, 2785–2835, doi:10.5194/bgd-6-2785-2009,
26 2009.
- 27 Woodrow, I. E. and Berry, J. A.: Enzymatic regulation of photosynthetic CO₂ fixation in C₃ plants, *Annu. Rev.
28 Plant Physiol. Plant Mol. Biol.*, 39, 533–594, doi:10.1146/annurev.pp.39.060188.002533, 1988.
- 29 Yi, C., Ricciuto, D., Li, R., Wolbeck, J., Xu, X., Nilsson, M., Aires, L., Albertson, J. D., Amman, C., Arain, M.
30 A., de Araujo, A. C., Aubinet, M., Aurela, M., Barcza, Z., Barr, A., Berbigier, P., Beringer, J., Bernhofer, C.,
31 Black, A. T., Bolstad, P. V., Bosveld, F. C., Broadmeadow, M. S. J., Buchmann, N., Burns, S. P., Cellier, P.,
32 Chen, J., Chen, J., Ciais, P., Clement, R., Cook, B. D., Curtis, P. S., Dail, D. B., Dellwik, E., Delpierre, N.,
33 Desai, A. R., Dore, S., Dragoni, D., Drake, B. G., Dufrêne, E., Dunn, A., Elbers, J., Eugster, W., Falk, M.,
34 Feigenwinter, C., Flanagan, L. B., Foken, T., Frank, J., Fuhrer, J., Gianelle, D., Golstein, A., Goulden, M.,
35 Granier, A., Grunwald, T., Gu, L., Guo, H., Hammerle, A., Han, S., Hanan, N. P., Haszpra, L., Heinesch, B.,
36 Helfter, C., Hendriks, D., Hutley, L. B., Ibrom, A., Jacobs, C., Johansson, T., Jongen, M., Katul, G., Kiely, G.,
37 Klumpp, K., Knohl, A., Kolb, T., Kutsch, W. L., Laflleur, P., Laurila, T., Leuning, R., Lindroth, A., Liu, H.,
38 Loubet, B., Manca, G., Marek, M., Margolis, H. A., Martin, T. A., Massman, W. J., Matamala, R., Matteucci,
39 G., McCaughey, H., Merbold, L., Meyers, T., Migliavacca, M., Miglietta, F., Misson, L., Molder, M., Moncrieff,



- 1 J., Monson, R. K., Montagnani, L., Montes-Helu, M., Moors, E., Moureaux, C., et al.: Climate control of
- 2 terrestrial carbon exchange across biomes and continents, *Environ. Res. Lett.*, 5, 034007, doi:10.1088/1748-
- 3 9326/5/3/034007, 2010.
- 4 Zheng, D., Raymond, H. and Running, S. W.: A daily soil temperature model based on air temperature and
- 5 precipitation for continental applications, *Clim. Res.*, 2, 183–191, doi:10.3354/cr002183, 1993.
- 6

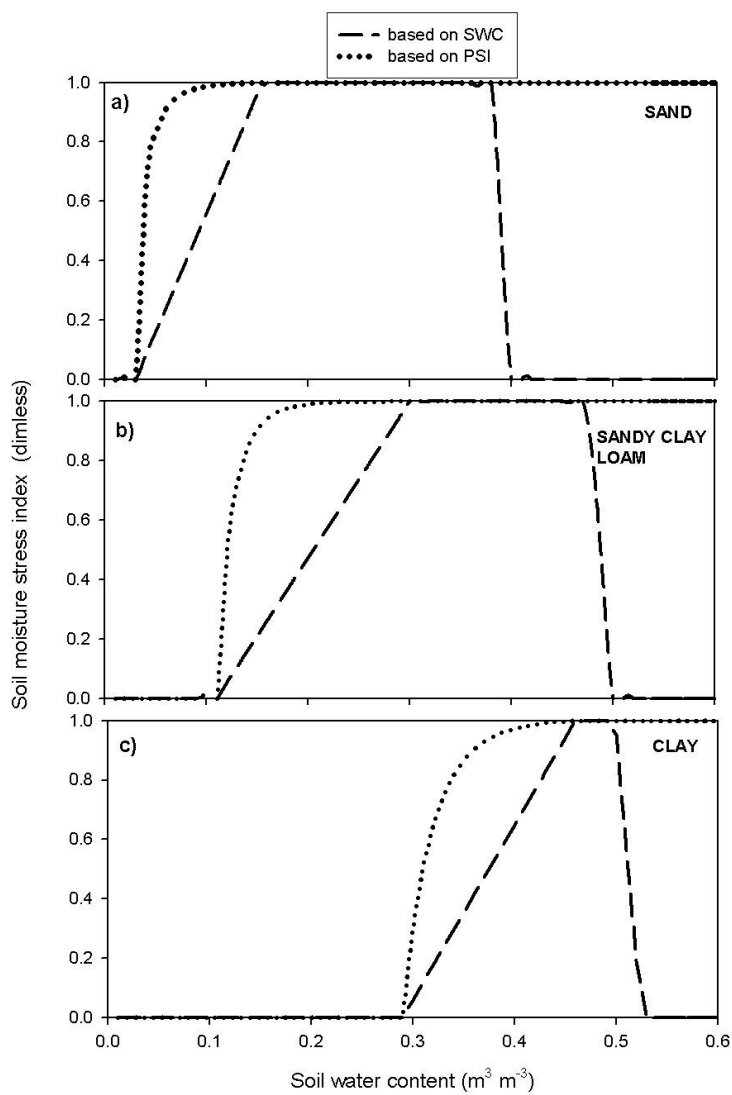


1

2

3

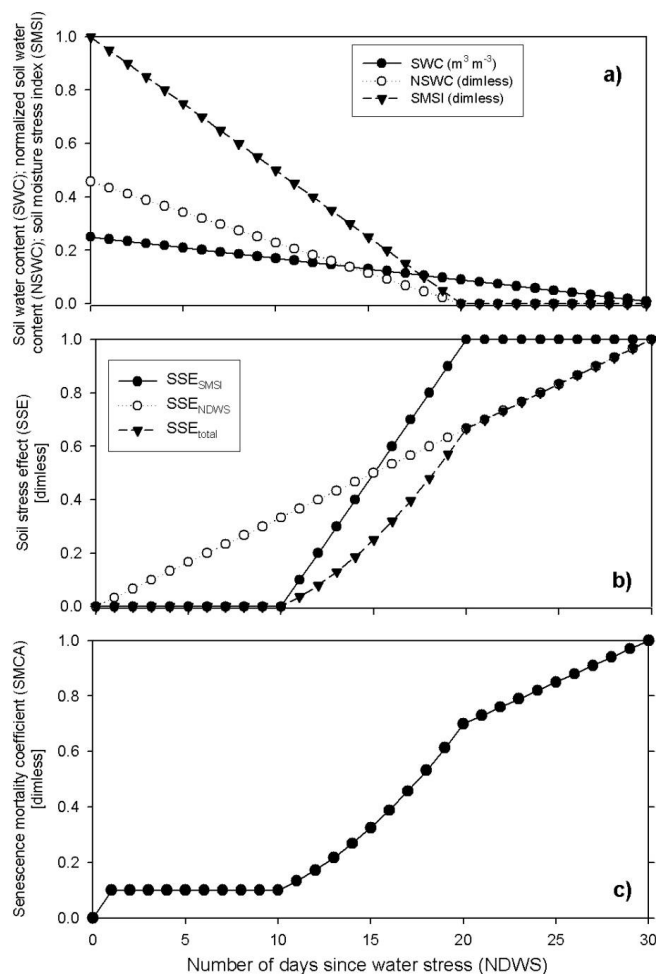
Figure 1. Dependence of normalized soil water content (upper part) and soil water potential (lower part) on soil water content in case of three different soil types.



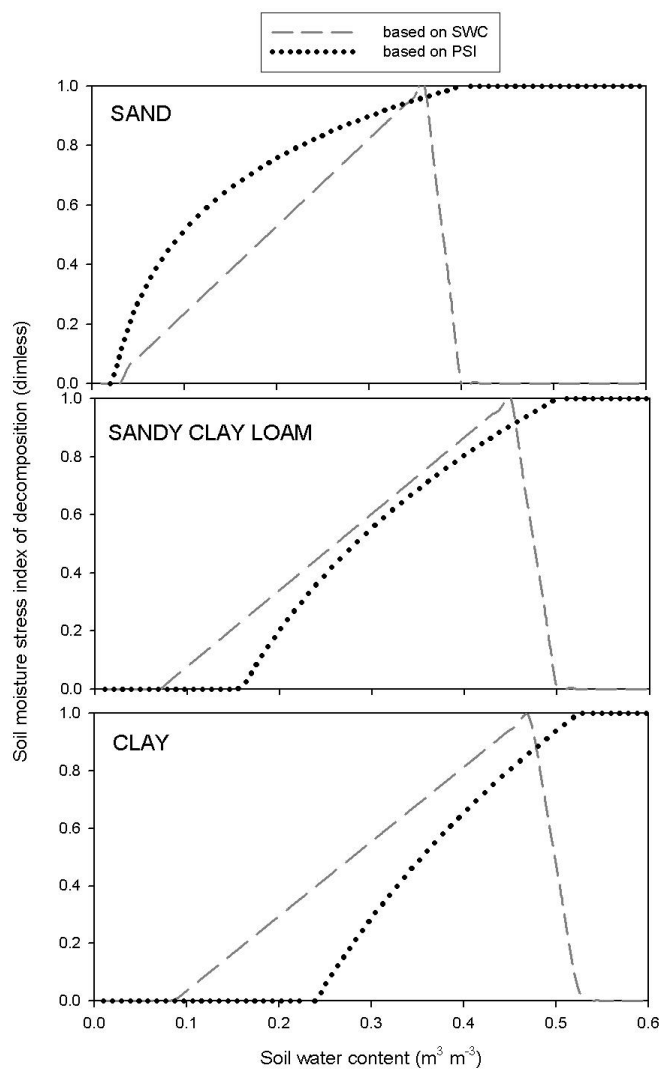
1

2 **Figure 2. Dependence of the soil moisture stress index on soil water content for three different soil types: sand (a),**
3 **sandy clay soil (b) and clay (c). Soil stress index based on soil water potential (dotted lines) is used by the original**
4 **model, while soil stress index based on normalized soil water content is used by BBGCMuSo (dashed lines).**

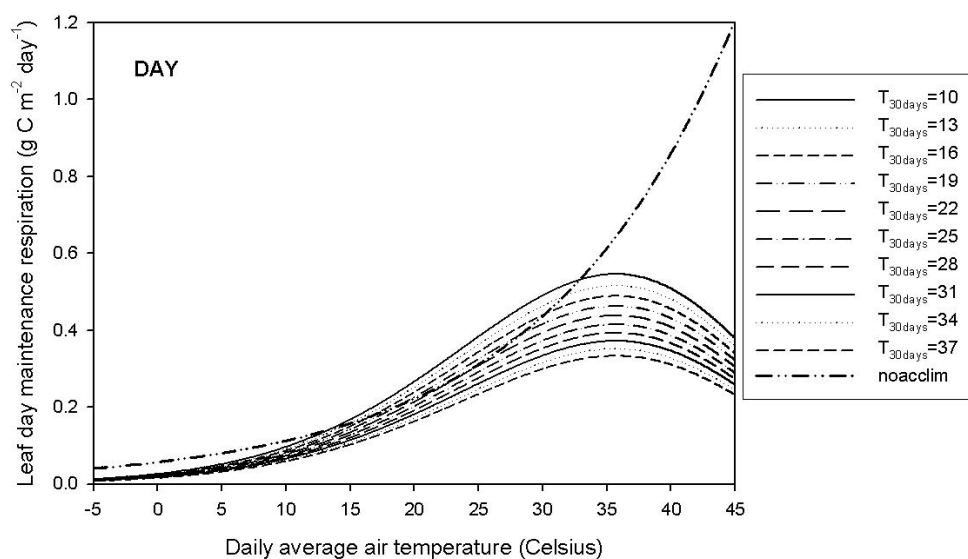
5



1
 2 **Figure 3. Demonstration of the senescence calculation with an example. a) Soil water content (SWC; black dots),**
 3 **normalized soil water content (NSWC; white dots) and soil moisture stress index (SMSI; black triangles) during 30**
 4 **days of a hypothetical drought event. b) Soil stress effect based on soil moisture stress index (SSE_{SMSI} ; black dots), soil**
 5 **stress effect based on number of days since water stress (SSE_{NDWS}) and total soil stress effect (SSE_{total}). c)**
 6 **Aboveground senescence mortality coefficient (SMCA).**

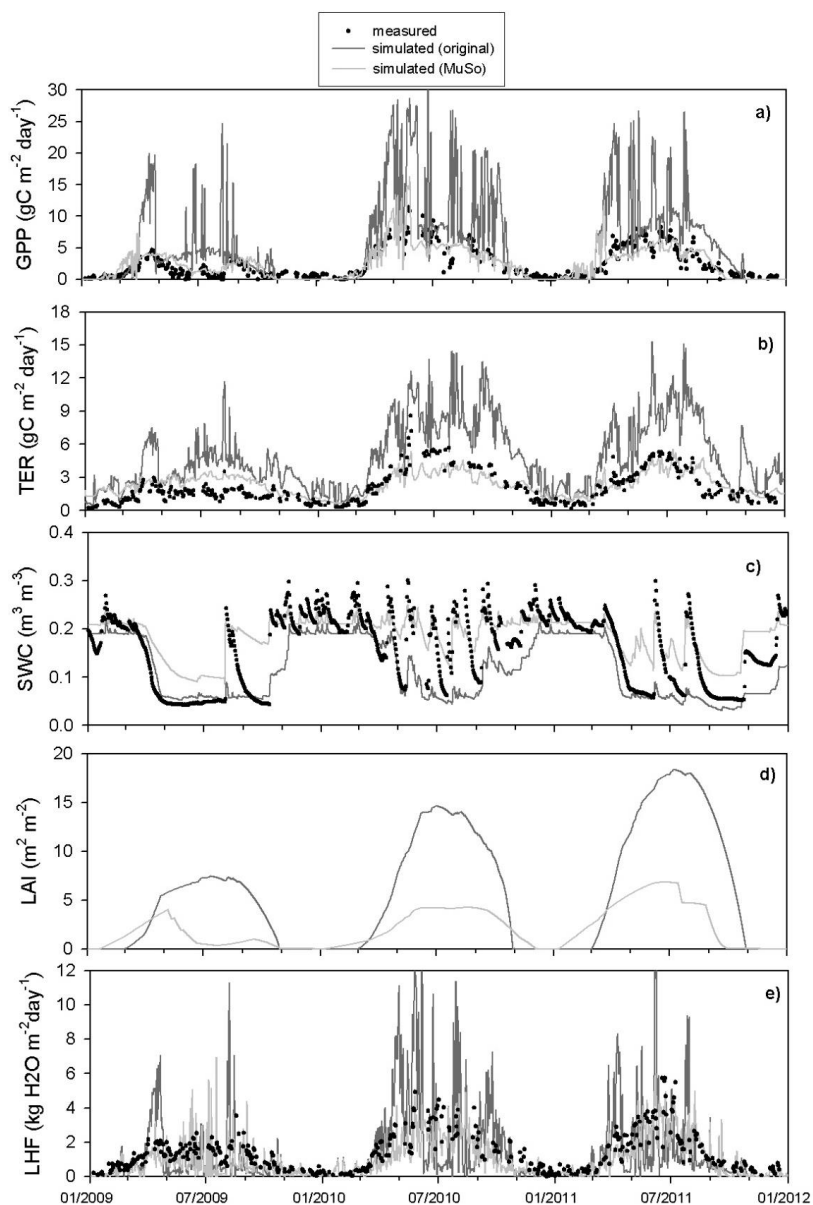


1
2 Figure 4. Soil moisture stress index used by decomposition for three different soil types: sand (a), sandy clay soil (b)
3 and clay (c). Soil stress index based on soil water potential (dotted lines) is used by the original model, while soil stress
4 index based on soil water content is used by BBGCMuSo (dashed grey lines).
5



1
2
3
4
5
6
7

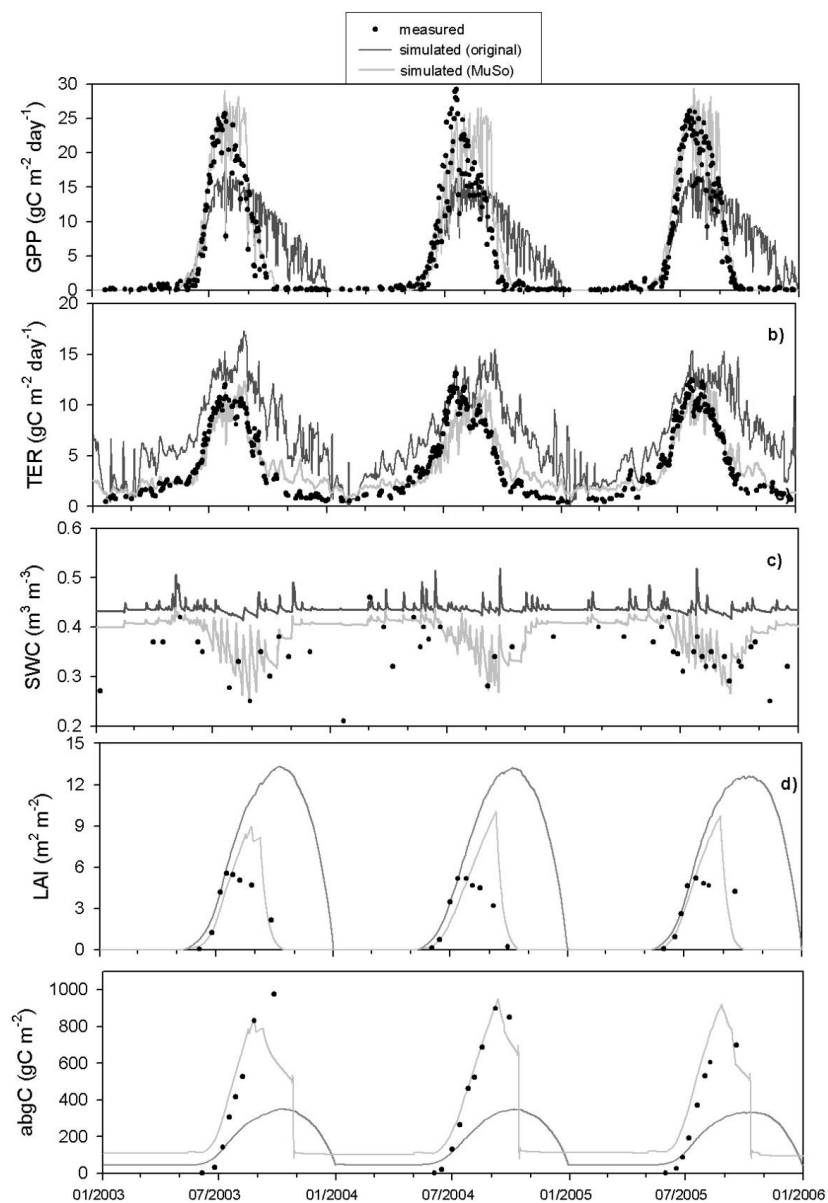
Figure 5. Acclimated and non-acclimated (noacclim) daytime maintenance respiration of leaf as a function of air temperature. Acclimated respiration values were calculated based on different average daily temperatures during the previous 30 days ($T_{30\text{days}}$: 10, 13, 16, 19, 22, 25, 28, 31, 34, and 37 Celsius). In case without acclimation, the respiration is independent of average daily temperature, therefore only one line is presented (this refers to the original model logic).



1

2 **Figure 6.** Measured (black dots) and simulated variables (a) GPP, b) TER, c) SWC, d) LAI, e) LHF using the original
3 Biome-BGC (dark grey lines) and BBGCMuSo (light grey lines) models for grassland at the Bugac site between 2009
4 and 2011. Measured LAI was not available at Bugac.

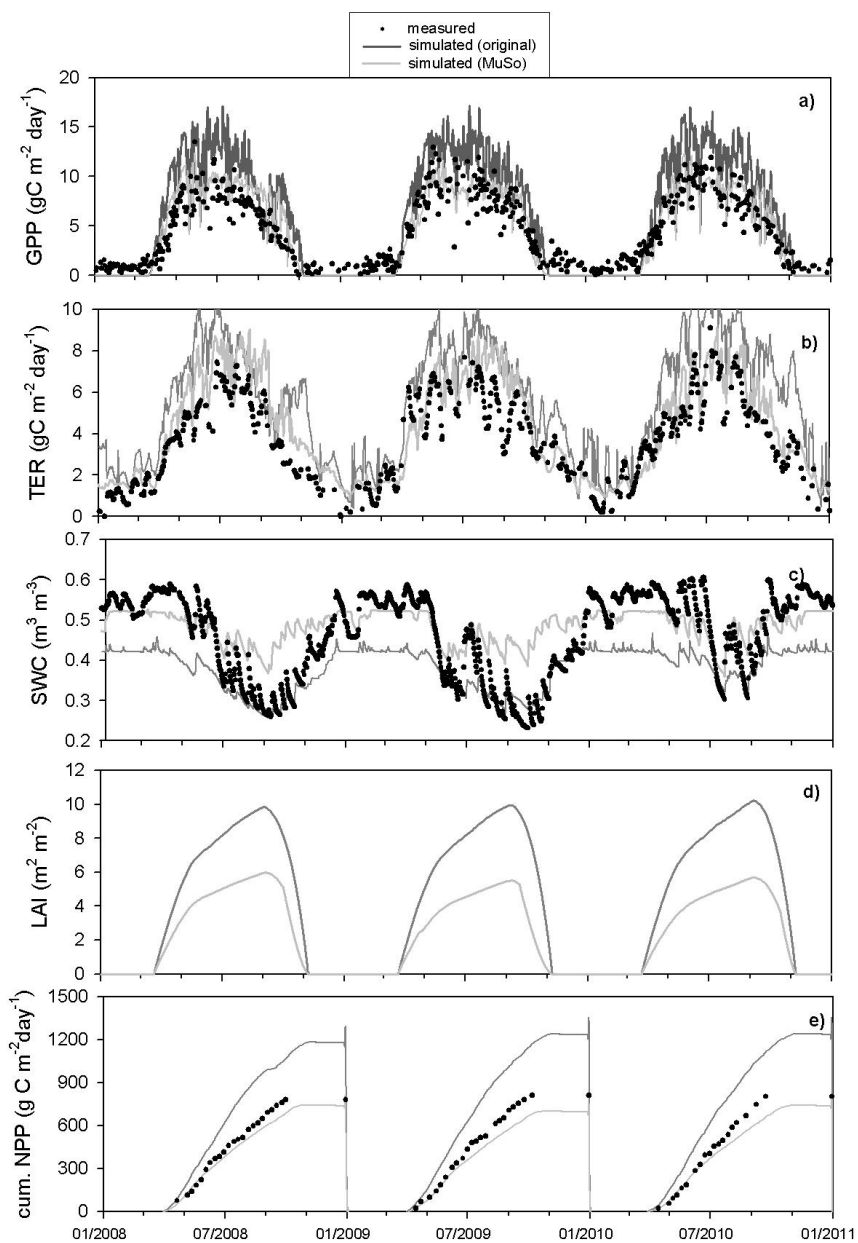
5



1

2 **Figure 7. Measured (black dots) and simulated variables (a) GPP, b) TER, c) SWC, d) LAI, e) abgC using original**
3 **Biome-BGC (dark grey lines) and BBGCMuSo (light grey lines) models for maize simulation at the Mead1 site,**
4 **between 2003 and 2006.**

5



1

2 Figure 8. Measured (black dots) and simulated variables using original Biome-BGC (dark grey lines) and
3 BBGCMuSo (light grey lines) regarding deciduous broad-leaved forest at the Jastrebarsko site between 2008 and
4 2010. a) GPP, b) TER, c) SWC (note: original Biome-BGC provides simulation results only for one layer, namely 'the
5 rooting depth', which is 0-100 cm in this case), d) LAI, e) cumulative NPP. Note that measured LAI is not available.

6



1 **Table 1: Summary of model adjustments. Group refers to major processes represented by collection of modules in**
2 **Biome-BGCMuSo, while sub-group refers to specific features.**

Group	Sub-group	Description
Multilayer soil	Thermodynamics	Two methods to calculate soil temperature layer by layer: logarithmic and the Ritchie (1998) method
	Hydrology	Calculation of soil water content and soil properties layer by layer. New processes: percolation, diffusion, runoff, diffusion, and pond water formation.
	Root distribution	Calculation of root mass proportion layer by layer based on empirical function after Jarvis (1989)
	Nitrogen budget	Instead of uniform distribution, calculation of soil mineral nitrogen content layer by layer
	Soil moisture tress index	Soil moisture stress index based on normalized soil water content calculated layer by layer
	Senescence	Senescence calculation based on soil moisture stress index and the number of days since stress is present
	Decomposition and respiration	Maintenance root respiration flux is calculated layer by layer. Limitation of soil moisture stress index.
Management	Management modules	Mowing, grazing, harvest, ploughing, fertilization, plating, thinning, and irrigation. 7 different events for each management activity can be defined per year, even in annually varying fashion.
	Management related plant mortality	Rate of the belowground decrease to the mortality rate of the aboveground plant material can be set optionally
Other plant related processes	Phenology	Alternative model based phenology. Calculating start and end of vegetation period using heat sum index for growing season (extension of index in Jolly et al., 2005)
	Genetically programmed leaf senescence	Genetically programmed leaf senescence due to the age of the plant tissue
	New plant pools	Fruit and soft stem
	C ₄ photosynthesis	Enzyme-driven C ₄ photosynthesis routine based on the work of Di Vittorio et al. (2010)
	Acclimation	Photosynthesis and respiration acclimation of plants, temperature-dependent Q ₁₀ (Smith and Dukes, 2012)
	LAI-dependent albedo	LAI-dependent albedo estimation based on the method of Ritchie (1998)
Model run	Stomatal conductance regulation	CO ₂ concentration is taken into account in stomatal conductance estimation based on the Franks et al. (2013)
	Dynamic mortality	Ecophysiological parameter for whole-plant mortality fraction can be defined year by year
	Transient run	Optional third model phase to enable smooth transition from the spinup phase to the normal phase
Methane and nitrous oxide soil efflux	Possibility of land-use-change simulation	Avoiding frequent model crash in case of different ecophysiological parameters set in spinup and normal simulations
	Unmanaged soils	Empirical estimation based on Hashimoto et al. (2011)
	Grazing and fertilization	Empirical estimation based on IPCC (2006) Tier 1 method

3

4



1 **Table 2. Default values of parameters in BBGCMuSo for different soil types. Soil types are identified based on the**
 2 **used-defined sand, silt and clay fraction of the soil layers based on the soil triangle method.**

	SAND	LOAMY SAND	SANDY LOAM	SANDY CLAY	SANDY CLAY LOAM	LOAM	SILT LOAM	SILT	SILTY CLAY LOAM	CLAY LOAM	SILTY CLAY	CLAY
B	3.45	10.45	9.22	5.26	4.02	50	7.71	7.63	6.12	5.39	4.11	12.46
SWC _{sat}	0.4	0.52	0.515	0.44	0.49	0.51	0.505	0.5	0.46	0.48	0.42	0.525
SWC _{fc}	0.155	0.445	0.435	0.25	0.38	0.42	0.405	0.39	0.31	0.36	0.19	0.46
SWC _{wp}	0.03	0.275	0.26	0.09	0.19	0.24	0.22	0.205	0.13	0.17	0.05	0.29
BD	1.60	1.4	1.42	1.56	1.5	1.44	1.46	1.48	1.54	1.52	1.58	1.38
RCN	50	70	68	54	56	64	66	62	58	60	52	72

3 B [dimensionless]: Clapp-Hornberger parameter; SWC_{sat}, SWC_{fc}, SWC_{wp} [m³ m⁻³]: SWCs at saturation, at the
 4 field capacity and at the wilting point, respectively; BD [g cm⁻³]: bulk density; RCN [dimensionless]: runoff
 5 curve number.
 6



1 **Table 3. Quantitative evaluation of the original and adjusted models at the grassland site in Bugac using different**
 2 **error metrics. ORIG means the original Biome-BGC, while MuSo refers the BBGCMuSo. See text for the definition of**
 3 **the error metrics.**

	R²		RMSE		NRMSE		NSE		BIAS	
	ORIG	MuSo	ORIG	MuSo	ORIG	MuSo	ORIG	MuSo	ORIG	MuSo
GPP	0.50	0.66	5.82	1.52	51.2	13.4	-4.78	0.61	2.81	0.11
TER	0.65	0.64	3.21	0.98	38.1	11.6	-3.59	0.57	2.47	0.33
LHF	0.24	0.62	1.89	0.83	33.2	14.5	-1.51	0.52	0.01	-0.33
SWC	0.60*	0.64	0.04*	0.09	34.6*	87.7	-0.46*	-8.3	-0.01*	0.09

4 *SWC simulated by the original Biome-BGC represents constant value within the entire root zone

5



1 **Table 4: Quantitative model evaluation regarding to maize simulation at the Mead1 site using different error metrics.**
 2 **ORIG** means the original Biome-BGC, while **MuSo** refers to the BBGCMuSo. See text for the definition on the error
 3 metrics.

	R²		RMSE		NRMSE		NSE		BIAS	
	ORIG	MuSo	ORIG	MuSo	ORIG	MuSo	ORIG	MuSo	ORIG	MuSo
GPP	0.61	0.87	5.83	3.44	19.0	11.1	0.58	0.86	-0.41	-0.91
TER	0.59	0.86	4.65	1.75	35.4	13.3	-0.58	0.78	3.8	-0.83
SWC	0.12*	0.01	0.13*	0.09	41.2*	30.1	-4.53*	-1.94	0.12*	0.07
LAI	0.26	0.59	5.81	1.61	97.6	27.1	-7.03	0.91	4.22	-0.01
agbC	0.36	0.82	296.5	159.6	27.4	14.8	0.17	0.76	-129.1	7.9

4 * SWC simulated by the original Biome-BGC represents constant value within the entire root zone

5



1 **Table 5: Quantitative model evaluation of simulation for deciduous broad-leaved forest for the Jastrebarsko forest**
 2 **site using different error metrics. ORIG means the original Biome-BGC, while MuSo refers to the BBGCMuSo. See**
 3 **text for the definition on the error metrics.**

	R²		RMSE		NRMSE		NSE		BIAS	
	ORIG	MuSo	ORIG	MuSo	ORIG	MuSo	ORIG	MuSo	ORIG	MuSo
GPP	0.84	0.84	3.67	1.77	27.3	13.1	-0.13	0.74	2.27	0.33
TER	0.81	0.83	2.5	1.31	27.4	14.4	-0.51	0.59	2.13	0.82
SWC	0.83*	0.67	0.11*	0.08	27.1*	21.2	0.06*	0.42	-0.08*	0.02
NPP	0.99	0.99	240.9	70.3	30.5	8.9	-0.03	0.91	220.3	-52.3

4 * SWC simulated by the original Biome-BGC represents constant value within the entire root zone